378 *Chem. Mater.* **2011,** *23,* 378–396
DOI:10.1021/cm102117c

CHEMISTRY OF MATERIALS
Review

Discotic Liquid Crystals for Opto-Electronic Applications[†,‡]

Bilal R. Kaafarani*

Department of Chemistry, American University of Beirut, Beirut 1107-2020, Lebanon

Received July 29, 2010. Revised Manuscript Received November 5, 2010

Discotic liquid crystals (DLCs) have been exploited in opto-electronic devices for their advantageous properties including long-range self-assembling, self-healing, ease of processing, solubility in a variety of organic solvents, and high charge-carrier mobilities along the stacking axis. An overview of DLCs and their charge-carrier mobilities, theoretical modeling, alignment, and device applications is addressed herein. The effects of alignment on charge-carrier properties of DLCs are discussed. Particular attention is devoted to processing techniques that achieve suitable alignment of DLCs for efficient electronic devices such as zone-casting, zone melting, Langmuir−Blodgett deposition, solution-casting on preoriented polytetrafluoroethylene (PTFE), surface treatment, IR irradiation, application of a magnetic field, use of sacrificial layers, use of blends, application of an electric field, and others.

1. Introduction

Since their discovery by Chandrasekhar[1] in 1977, discotic liquid crystals (DLCs) have attracted the attention of many research groups. Serious efforts have been made to exploit DLCs in organic electronic devices. A typical discotic mesogen generally includes a central aromatic core functionalized with three to eight flexible chains. The two main types of mesophases DLCs form are nematic and columnar. In the nematic phase, discs have orientational order while in the columnar phase the discs pile into columns, see Figure 1, and are generally considered most useful for organic electronics applications.[2] A comprehensive review of the chemical aspects of DLCs was reported by S. Kumar,[3] wherein the existence of six different columnar DLC phases: hexagonal columnar, rectangular columnar, columnar oblique, columnar plastic, helical, and columnar lamellar, are reported.[3] On the other hand, indenes and pseudoazulenes were the first reported thermotropic DLCs that do not bear flexible chains.[4] Moreover, DLCs with shape-persistent macrocylic cores were also reported.[5]

Several review articles have addressed the design and important features of DLCs.[2,3,5−19] In consideration of the increased interest in DLCs, this review not only focuses on the specific aspects of DLCs for potential use in opto-electronic devices but also highlights recent progress in the development of DLCs of promising performance in electronic devices. Scrupulous attention is devoted to alignment techniques of DLCs that improve such performance. Moreover, additional developments posterior to the 2006−2007 seminal reviews by Geerts,[14] Kumar,[3] and Laschat[13] are particularly highlighted.

DLCs may form efficient $\pi-\pi$ columnar stacks that produce high charge-carrier mobilities, the magnitude of which is fundamentally determined by the degree of order and $\pi-\pi$ molecular orbital overlap within the columnar stacks. Charge transport within the stack, i.e., in a one-dimensional manner, is therefore built into the design scheme. The ease of film formation is another key feature of smart materials for organic-based electronic and optoelectronic devices. Because some DLCs have a predisposition to self-assemble into columnar stacks, ease of processability is inherent, although orientation of the columnar stacks in the direction required for the device function can be challenging. Furthermore, because of their liquid-character, DLCs possess the capacity to self-heal structural defects such as grain boundaries and consequently have the ability of attaining several square millimeters large single domains of several micrometers film thickness.[14] The advantageous properties of DLCs, therefore, include long-range self-assembling (order), self-healing (dynamics), ease of processing, high solubility in organic solvents, and high charge-carrier mobility.

The driving force for formation of columnar mesophases has been postulated to be shape anisotropy,[4,20,21] microsegregation between flexible chains and rigid core,[22] and core−core van der Walls attractions.[2] The core−core distance along the column direction is usually in the order of 3.5 Å whereas the distances between the centers of cores in adjacent columns is dictated by the size of the mesogens and is typically of the order of 20−40 Å. Flexible alkyl chains around the cores substantially insulate the column from the neighboring column. Conductivity is, therefore, anticipated to be significantly higher along the column axis; therefore, the DLC columns are sometimes referred to as quasi-one-dimensional

[†] Accepted as part of the "Special Issue on π-Functional Materials".
[‡] This paper is dedicated to Prof. Makhlouf J. Haddadin on the occasion of his 75th birthday.
*To whom correspondence should be addressed. E-mail: bilal.kaafarani@aub.edu.lb.

 Published on Web 11/24/2010

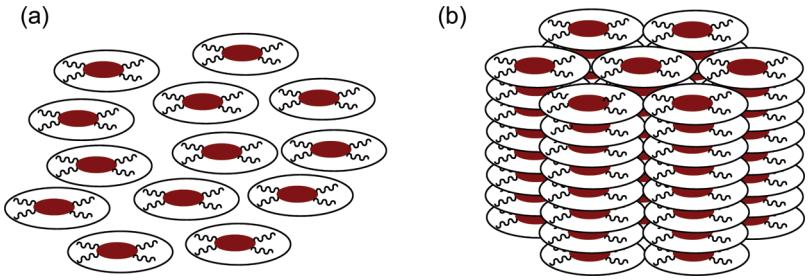

Figure 1. Schematic representations of (a) the discotic nematic and (b) the columnar phase.[2] Modified version of Figure 1 from the article: Kumar, S. *Liq. Cryst.* **2004**, *31*, 1037−1059. Reprinted by permission of the publisher (Taylor & Francis Group, http://www.informaworld.com).

conducting wires.[2] On the other hand, calamatic liquid-crystals exhibit two-dimensional charge transport analogous to that observed in pentacene and oligothiophene, which demonstrate herringbone packing.[14,23] Moreover, the orbital overlap in DLCs is much larger than that of calamatics.[24]

The structure of the conjugated core of the discoid materials govern their molecular-level electronic properties, whereas the change in the peripheral flexible chains and aromatic cores control their self-assembly in both solution and bulk phase; the overall electronic properties of the materials, therefore, depend on both core and substituent structure.[25] The supramolecular assembly of DLC materials can also be strongly affected by the processing method.[25]

In this review, a short overview of DLCs, their charge mobilities, and their mesophase engineering is first addressed. This is followed by highlighting a particular aspect associated with DLCs, i.e., alignment. The different processing techniques to achieve suitable alignment for an efficient device (OFET, OLED, OPV) are discussed.

2. Overview of DLCs

Discotic liquid crystals have been reported with a large number of discoid cores including benzene,[26−30] pyridine,[31] triazine,[28,30,32] triphenylene,[2,12] diazatriphenylene,[33] hexaazatriphenylene,[34] pyrene,[35] dibenzo[*g*,*p*]chrysene,[36,37] dibenzonapthacene,[38] tristriazolotriazine,[39] rufigallol,[40−42] truxene,[43] triazatruxene,[44] or triindole,[45] tricycloquinazoline,[46,47] hexaazatrinaphthylene (HATNA),[48,49] perylene,[50] coronene diimide,[51] phthalocyanine (Pc),[52−56] porphyrin,[57,58] quinoxalinophenanthrophenazine (TQPP),[59,60] pyrazinopyrazinoquinoxalinophenanthrophenazine (TPPQPP),[60] dodecaazatrianthracene (DATAN),[60] and hexa-*peri*-hexabenzocoronene (HBC),[61] see Figure 2. Müllen's group has recently reported DLCs of large aromatic polycyclic hydrocarbons cores paving the road to stimulating research developments in the field of organic electronics such as the synthesis of thin graphene layers, see Figure 2.[62,63]

The nature of the discoid core and flexible chains affect the self-assembly of DLCs.[25] Some examples are herein briefly illustrated. The substitution of hexaazatriphenylene with six alkyl or alkylthio groups does not result in columnar mesophases,[34] but the addition of H-bonding side groups induces mesophase behavior.[64] Recently, Armstrong's group reported the self-organization of a phthalocyanine derivative into columnar aggregates, which were attributed to the H-bonding interactions between the benzamide groups of the side chains, see Figure 3.[65] Computational simulations attribute such behavior to the intermolecular electrostatic potential among the discoid cores; this is a crucial factor in stabilizing/destabilizing the columnar phases.[66] The self-assembly of HBC derivatives was further enhanced upon the introduction of H-bonding side groups to the core.[67] The change in position of functional group (carboxylic acid, methyl carboxylate, or nitro group) in a series of dibenzophenazine DLCs from the "top" to the "side" of the aromatic core strongly affects their stability and mesophases.[68] The effect of symmetry on the stability of columnar phase in dibenzophenazine and triphenylene derivatives was also studied wherein the melting temperatures of less symmetrical DLCs were found to be lowered by a much larger degree than clearing temperatures.[69] On the other hand, the substitution of the discoid core with electron-withdrawing groups stabilize the mesophases and increase the fluorescence quantum yield.[70]

3. Charge-Carrier Mobilities

The mobility of charge carriers in organic semiconducting materials may determine their suitability for use in electronic devices. In crystalline materials, the mobility is strongly influenced by the properties of the solid state. In comparison to amorphous materials, single crystals of high-purity of planar organic compounds (such as the acenes, i.e., anthracene, pentacene) show higher mobility due to their well-organized stacking behavior. While staggeringly high mobilities have been reported in single crystal-devices, the major drawbacks in this approach are both the cost and time-effort associated with the growth of single crystals. Workers generally target systems programmed to self-assemble under wet-processing conditions. The mobility ultimately controls the switching speed of the field-effect transistor, the intensity of the light emitting diode, and the separation of charges in photovoltaic cells.[71]

Different techniques and geometries have been used to measure the mobility of charge-carriers in DLC materials. These include the pulse radiolysis time-resolved microwave conductivity technique (PR-TRMC),[72−78] time-of-flight (TOF),[79−82] steady-state space charge-limited current (SCLC),[83−86] and field-effect mobility.[87−89] PR-TRMC determines the mobility of charge-carriers at the local level and is relatively insensitive to defects

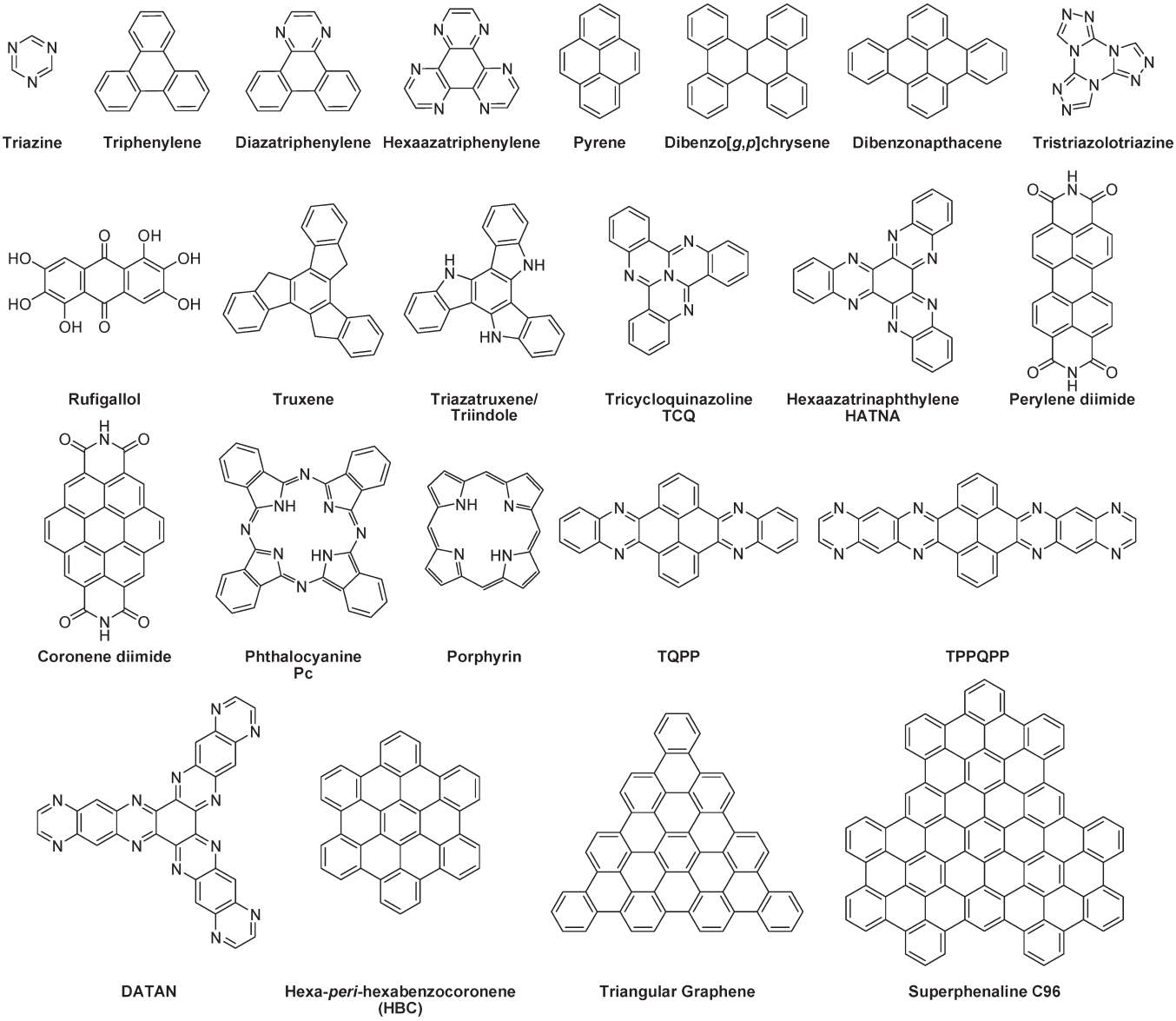

Figure 2. Selected aromatic cores used in discotic mesogens.

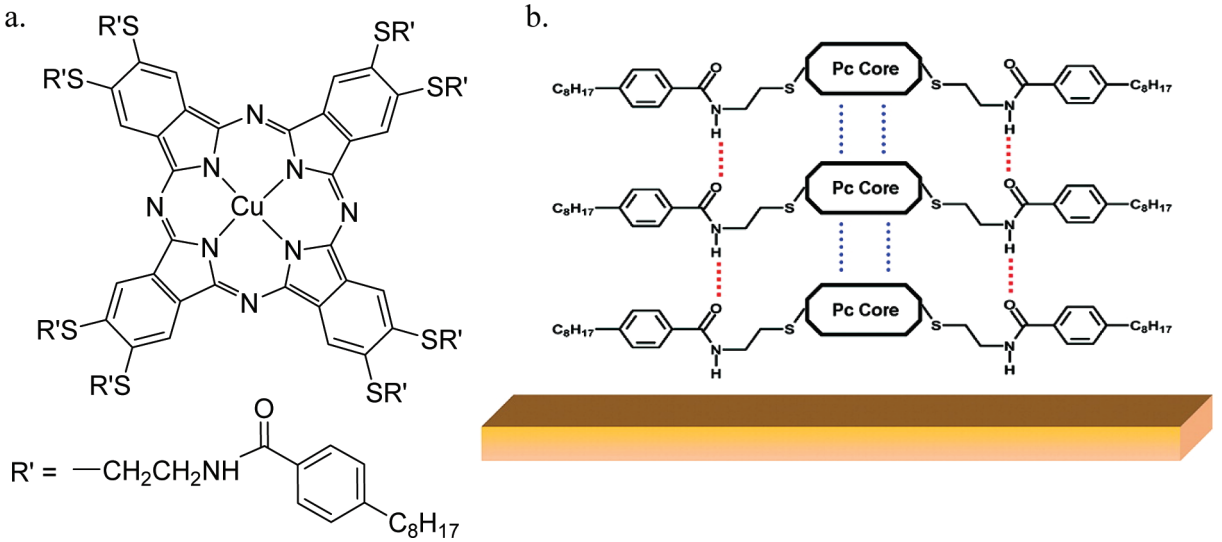

Figure 3. (a) Chemical structure of 2,3,9,10,16,17,23,24-octa(2-(4-octylbenzamide ethylsulfanyl) phthalocyanato copper(II). (b) Schematic view of the aggregation of the molecules through hydrogen bondings exerted via amide units in the side chains, $\pi-\pi$ stacking between the aromatic rings, and S−S interactions.[65] Reprinted from ref 65. Copyright 2010 American Chemical Society.

(shows mobility within spatial limited domains) or, in the case of 1D conductors such as columnar DLCs, to the orientation(s) of the column axes. Thus, the method often gives values larger than those seen on the macroscopic scale; on the other hand, it can be regarded as giving a measure of what might be achievable if defect-free well-aligned samples could be obtained. In contrast, TOF and field-effect mobilities measure the macroscopic values and are strongly dependent on the presence of defects.[15] SCLC mobility is calculated from the current−voltage characteristics of thin organic films sandwiched between injecting electrodes.[90] Recent review articles collected the TOF[15] and PR-TRMC[71,74] mobilities of selected discotics. Studies comparing mobilities using some of the aforementioned techniques were also reported.[74,90]

van de Craats and Warman reported that a lower charge mobility in the columnar hexagonal phase (Col_h) was generally observed when alkyl chains are connected to the core via an oxygen atom as opposed to those for which the chains are coupled either directly (i.e., via methylene moiety) or via a sulfur.[75] The authors developed eq 1, based on previous PR-TRMC experimental results on triphenylene, porphyrin, coronene monoimide, azocarboxyldiimido-perylene, phthalocyanine, and *peri*-hexabenzocoronene, to predict the maximum mobility.

$$\sum \mu_{max} \approx 3e^{-83/n}\ cm^2/V\ s \qquad (1)$$

where n is the total number of C, N, and O atoms in the core.[75]

However, Müllen's group showed that mobility values predicted in eq 1 are limited to core sizes of $n < 40$ in HBC derivatives.[77] The relationship between core size, side chain length, and supramolecular organization of polycyclic aromatic hydrocarbon (PAH) cores, ranging from 42-carbon HBC core to a larger PAH core of 132-carbon atoms, was also investigated by the Müllen's group.[91] The authors reported the lateral packing of PAH cores to increase with the molecular masses of the core, which form the columnar stacks, and of the side chains which fill the core periphery.[91]

In addition, the nature of the substituents linked to the discoid core may affect the solubility, supramolecular order, and thus the charge-carrier mobility of DLCs. Branching side chains closer to the point of attachment to the HBC results in a decrease of the isotropic temperature and the $\pi-\pi$ interaction between the discoids. However, the intramolecular order remains high at room temperature with charge-carrier mobility in the order of 0.73 $cm^2\ V^{-1}\ s^{-1}$.[92] Doping 2,3,6,7,11-(hexakishexyloxy)triphenylene (HAT6) with 1% (w/w) methylbenzenethiol-coated gold nanoparticles increased the conductivity in the Col_h phase by 3 orders of magnitude ($\sim 10^{-12}$ to $\sim 10^{-9}\ \Omega^{-1}\ cm^{-1}$), as well as in the crystalline and isotropic phases.[93] The authors also reported a further 3−4 orders of magnitude ($\sim 10^{-6}\ \Omega^{-1}\ cm^{-1}$) increase in conductivity upon the application of a field.[93] Such increase in conductivity is attributed to the formations of chains of gold nanoparticles.[93]

Recently, a saturation hole mobility of $10^{-3}\ cm^2\ V^{-1}\ s^{-1}$ was reported in TQPP-$[SC_{12}H_{25}]_4$,[89] which showed multiple crystalline phases, but no mesophase behavior was observed.[94] However, TQPP-$[t\text{-}Bu]_2$-$[OR]_4$ exhibited multiple DLC phases as observed by differential scanning calorimetry (DSC), polarized light microscopy (PLM), and wide-angle X-ray diffraction (WAXD); however, no charge-carrier mobilites have yet been reported on this series.[60]

The TOF hole mobility of hexapentyloxytriphenylene in the Col_h phase was reported to be temperature and electric-field dependent with charge-carrier mobilities up to $2 \times 10^{-3}\ cm^2\ V^{-1}\ s^{-1}$ at 85 °C. Drift velocity was reported to be linearly dependent on the electric field below 10^{-5} V/cm reaching saturation at higher fields.[95] On the other hand, hexahexylthiotriphenylene exhibited both electron and hole mobility in the order of 0.08 $cm^2\ V^{-1}\ s^{-1}$ in the helical Col_h phase at 45 °C.[96] A high SCLC hole mobility of 0.09 $cm^2\ V^{-1}\ s^{-1}$ was reported in 10,15-dihydro-5*H*-diindolo[3,2-*a*:3′,2′-*c*]-carbazole (indole) in its crystalline phase at 22 °C whereas the mobility in the Col_h phase decreased by a 3−4 factor.[45] The authors attributed the lower mobility in the Col_h phase to the higher motional freedom of the side chains and thus increasing the structural disorder in the columns.[45] An SCLC charge-carrier mobility as high as 1.3 $cm^2\ V^{-1}\ s^{-1}$ was reported for *N*,*N*′-di[3,4,5-tri(docecoxy)benzyl]-3,4,9,10-perylene diimide in its disordered columnar hexagonal phase (Col_{hd}) at room temperature.[50] The authors showed the strong dependence of SCLC mobilities on the morphology of the films which is itself affected by the processing technique.[50] TOF measurements of 1,3,6,8-tetrakis(3,4-dioctyloxyphenyl)pyrene indicated an ambipolar charge transport with mobility in the order of 10^{-3} $cm^2\ V^{-1}\ s^{-1}$ in its Col_h phase at 60 °C.[97] In addition, the TOF carrier mobility of molecular aligned DLC Cu-phthalocyanine was as high as $2.60 \times 10^{-3}\ cm^2\ V^{-1}\ s^{-1}$,[98] whereas a metal-free phthalocyanine DLC exhibited an OFET hole mobility up to $2.8 \times 10^{-3}\ cm^2\ V^{-1}\ s^{-1}$.[52] The gelation of 2,3,6,7,10,11-hexa(hexyloxy)triphenylene with hydrogen-bonded fibrous aggregates increased the hole mobility from 4.5×10^{-4} to $1.2 \times 10^{-3}\ cm^2\ V^{-1}\ s^{-1}$; the mobility was independent of temperature and electric field strength.[99] The columnar phase of a derivative of coronenedimide substituted with perfluorooctyl chains, obtained by cooling from isotropic phase, exhibited a remarkable SCLC electron mobility of 6.7 $cm^2\ V^{-1}\ s^{-1}$ at ambient temperature.[51] The H-bonding in hexacarboxamidohexaazatriphenylene (HAT-$CONHC_{12}H_{25}$] induced the columnar order in these discotics leading to an inter-disc distance of 3.18 Å with a $\sum\mu_{1D}$ values varying from 0.04 $cm^2\ V^{-1}\ s^{-1}$ at −80 °C to 0.08 $cm^2\ V^{-1}\ s^{-1}$ at 200 °C.[100] The Col_h mesophase of coronenemonoimide showed a mobility of 0.2 $cm^2\ V^{-1}\ s^{-1}$ at room temperature; this value increased gradually to 0.3 $cm^2\ V^{-1}\ s^{-1}$ just below the clearing temperature of 160 °C.[101]

Recently, Müllen's group reported the synthesis of a triangularly shaped polyaromatic hydrocarbon, see Figure 4, of 3-fold symmetry leading to a helical packing structure and 60° rotation angle and therefore forming the optimal local arrangement for charge transport.

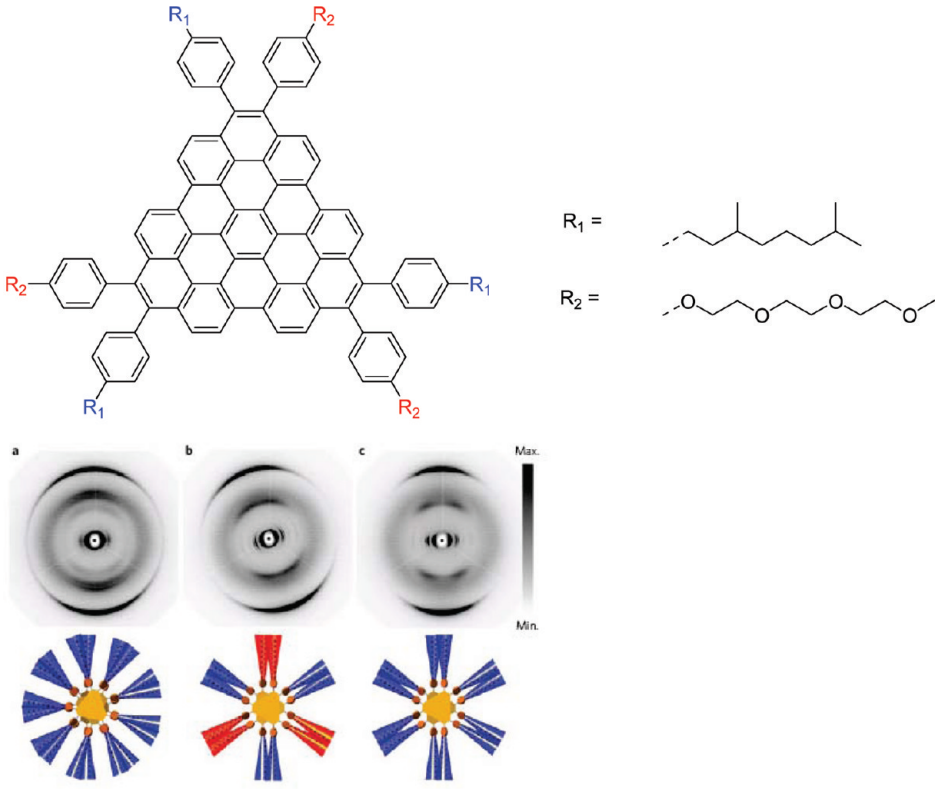

Figure 4. Two-dimensional wide-angle X-ray scaterring patterns and corresponding schematic illustrations of top-viewed triangularly shaped polyaromatic hydrocarbon molecules stacked on top of one another.[102] Reprinted by permission from Macmillan Publishers Ltd: Feng, X.; Marcon, V.; Pisula, W.; Hansen, M. R.; Kirkpatrick, J.; Grozema, F.; Andrienko, D.; Kremer, K.; Müllen, K. *Nat. Mater.* **2009**, *8*, 421−426, copyright (2009).

PR-TRMC measurements of this compound showed a mobility of 0.2 $cm^2\ V^{-1}\ s^{-1}$.[102] The authors argued that mobility is limited by structural defects and that an ideal defect-free assembly of materials may lead to a mobility up to 15 $cm^2\ V^{-1}\ s^{-1}$.[102]

Finally, Wöll and co-workers lately presented evidence for bandlike transport of electrons in highly ordered self-assembled monolayers (SAMs) of HBC materials anchored to Au substrate via S−Au bonds.[103] The authors proposed that the poor charge-carrier mobilities, which are governed by lateral hopping transport, increase considerably in the presence of a high degree of molecular ordering with estimated electron mobilities in the order of 5 $cm^2\ V^{-1}\ s^{-1}$ at 300 K within highly ordered HBC-based SAMs.[103]

The aforementioned synopsis of charge-carrier mobilities of selected DLCs demonstrates the prospective of designing a DLC of high charge-carrier mobility. The challenge remains producing defect-free films over large areas for DLCs exhibiting high charge-carrier mobility.

4. Transition and Mesophase Engineering

Researchers were also able to engineer DLC mesophases via different approaches. Aida's group reported the controlled self-assembly of amphiphilic HBC derivatives.[104−107] Amphiphilic HBC derivatives substituted with trinitrofluorene (TNF) moieties form coaxial nanotubular structure (16 nm in diameter and several micrometers long), wherein the electron-donating graphitic layer of π-stacked HBC are coated by a layer of the electron-accepting TNF, allowing photochemical generation of charge-carriers and a rapid photoconductive response with an on/off ratio larger than 10^4.[104] Electron-rich discoids when doped with TNF may form charge-transfer (CT) complexes leading to supramolecular assemblies and mesophases. Such CT complexes were reported in 1:1 mixtures of pentakis(phenylethynyl)phenol and TNF and resulted in different mesophases with higher clearing temperature.[108] The addition of a series of trinitrofluorene-based acceptors to a discotic mesogen carrying five methoxy groups and one functional tail (see Figure 5) has led to CT complexes of a wide range of mesophase behavior.[109] The interaction of mulityne DLC with TNF was studied using deuterium NMR by measuring the peaks quadrupolar splitting. This provides information about the orientational order of the complex of the deuterated compounds.[110]

The introduction of a lateral nuclear dipole moment in 1,4-difluoro-2,3,6,7,10,11-hexakis(hexyloxy)triphenylene (2F-HAT6), see Figure 6, resulted in a Col_h mesophase from below room temperature to 121 °C as opposed to a Col_h mesophase between 70 and 100 °C in HAT6.[111] This has increased the TOF mobility from 7.1×10^{-4} $cm^2\ V^{-1}\ s^{-1}$ in HAT6 to 1.6×10^{-3} $cm^2\ V^{-1}\ s^{-1}$ in 2F-HAT6. The authors also reported the increase of the TOF mobility to 1.5×10^{-2} $cm^2\ V^{-1}\ s^{-1}$ in a 1:1 stoichiometric mixture of 2F-HAT6 and 2,3,6,7,10,11-hexakis-(4-nonylphenyl)triphenylene (PTP9).[111]

In addition, functionalizing fluorinated dendrons at their ends with different electron donor (D) and acceptor (A) groups, see Figure 7, self-assemble into supramolecular liquid crystals phases, which exhibit hole mobility up to

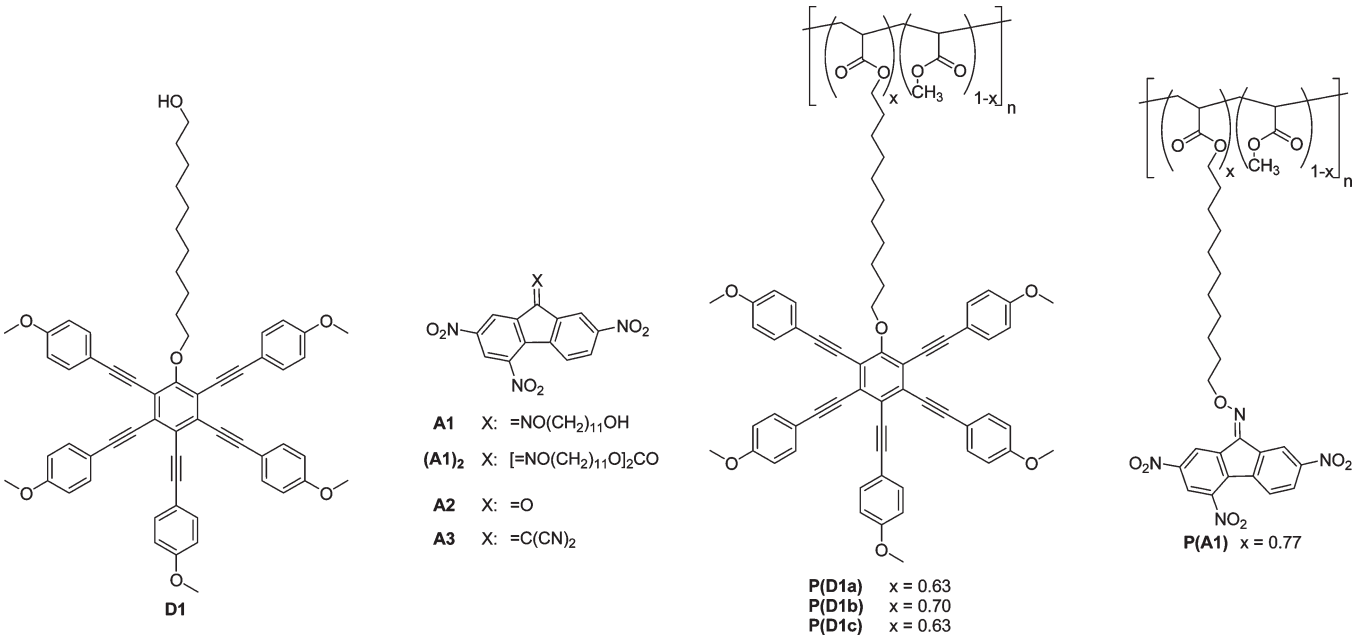

Figure 5. Studied materials.[109]

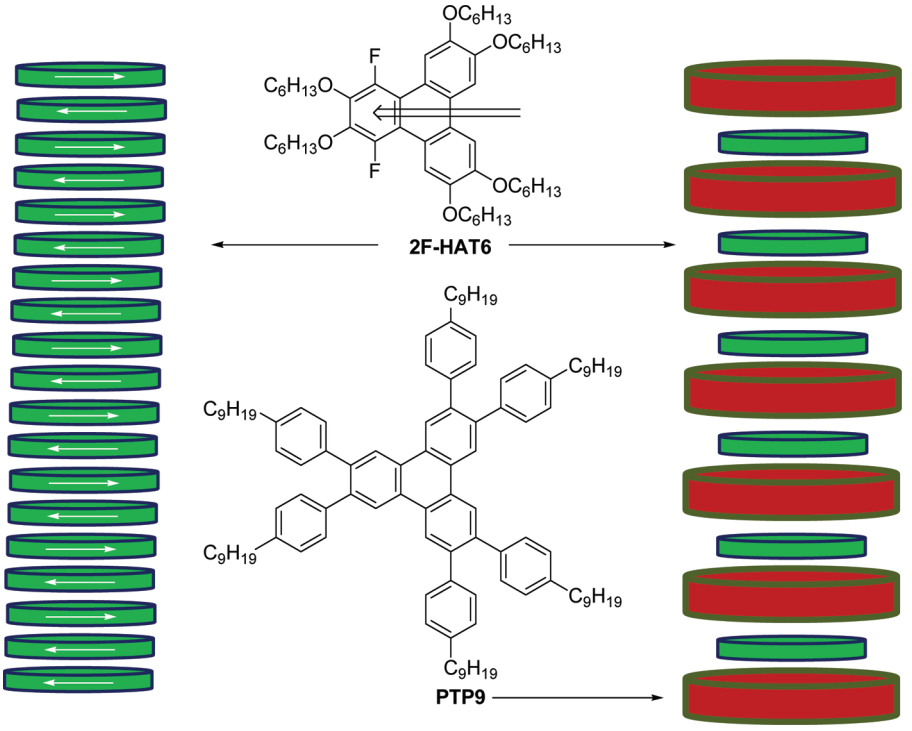

Figure 6. Schematic representation of the stabilization of a columnar phase through antiferroelectric alignment of molecular dipoles as in 2F-HAT6 or by formation of a CPI compound as in 2F-HAT6 + PTP9.[111] Modified version of Figure 2 from the article: Bushby, R. J.; Donovan, K. J.; Kreouzis, T.; Lozman, O. R. "Molecular engineering of triphenylene-based discotic liquid crystal conductors" *Opto-Electron. Rev.* **2005**, *13*, 269−279. Reproduced with permission.

10^{-3} cm^2 V^{-1} s^{-1} for the D-dendrons and electron mobility up to 10^{-3} cm^2 V^{-1} s^{-1} for the A-dendrons.[112]

Arene−perfluoroarene interactions were exploited to control the mesophase behavior of functionalized triphenylene monomers/polymers in a 1:1 mixture with perfluorotriphenylene.[113] The authors reported the stabilization of the DLC mesophase by perfluoroarene−arene interactions with an increase of 70 °C in the clearing temperature.[113]

Furthermore, doping triphenylene discotics with electron deficient ferrocenium ion formed a charge transfer complex leading to an increase in the charge-carrier mobility along the discoids without affecting the Col_h mesophase.[114] Blending HBC derivative with electron-donating perylenediimide and terrylenediimide derivatives led to a considerably higher level of order within the self-assembled columnar stacks.[115]

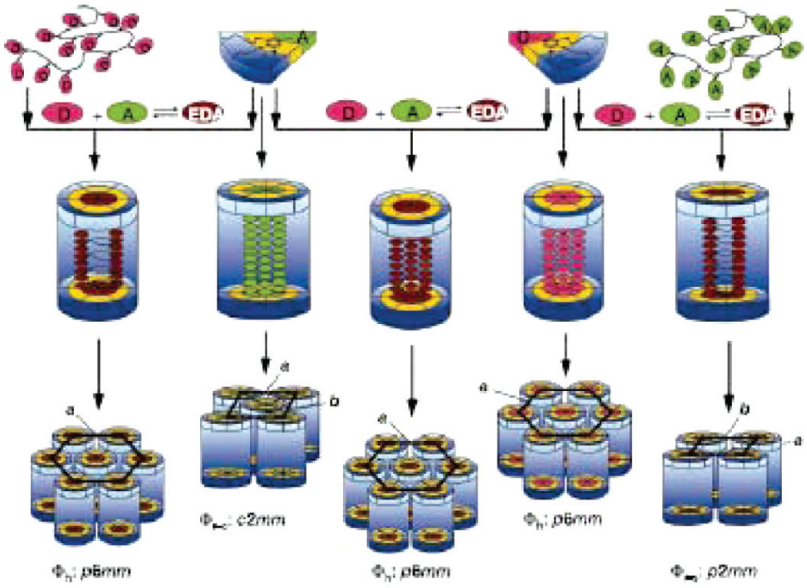

Figure 7. Schematic illustration of the LC assembly process in fluorinated dendrons functionalized at their tips with electron donor (D) and electron acceptor (A).[112] Reprinted by permission from Macmillan Publishers Ltd: Percec, V.; Glodde, M.; Bera, T. K.; Miura, Y.; Shiyanovskaya, I.; Singer, K. D.; Balagurusamy, V. S. K.; Heiney, P. A.; Schnell, I.; Rapp, A.; Spiess, H. W.; Hudson, S. D.; Duan, H. *Nature* **2002**, *419*, 384−387, copyright (2002).

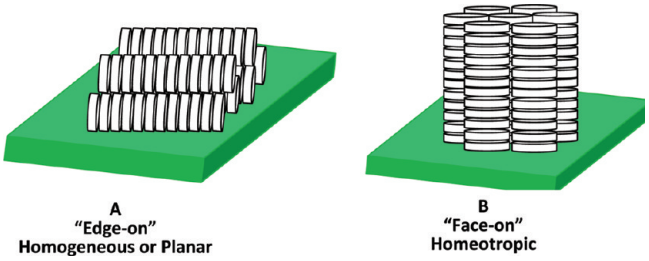

Figure 8. (A) "Edge-on", homogeneous, or planar unidirectional alignment; (B) "face-on" or homeotropic alignment.

5. Alignments

There are two distinct alignments of columnar DLCs: (a) homogeneous, edge-on or uniaxial planar (column axis parallel to a substrate) and (b) homeotropic or face-on (column axis perpendicular to a substrate), see Figure 8. Unidirectional planar alignment is ideal for OFETs while the homeotropic alignment is ideal for OPV or OLED applications.[116−118] For rectangular columnar ordered mesophases, Liu et al. proposed two limiting orientations of the molecular columns wherein the columns are either parallel or perpendicular to the substrate with a slight tilt.[119] Slow cooling of DLCs from the isotropic phase may lead to homeotropic alignment since the face-on orientation of the first molecular layers act as nucleation sites for the further self-assembly of discs perpendicular to the substrate.[120]

The ability to control the structural order and alignment of semiconducting materials is critical to attain high charge-carrier mobility.[121−123] A plethora of techniques has been used to align DLCs, some of which are described below in more detail.

5.1. Zone-Casting. Zone-casting allows alignment of organic materials in a homogeneous fashion. DLC material, dissolved in solvent, is continuously supplied through a nozzle on a moving substrate with a temperature gradient. Homogeneous alignment is achieved due to a concentration gradient in the meniscus formed between the nozzle and the moving substrate.With a change in the parameters of the casting (solvent, concentration, temperature, nozzle/substrate distance, rate of supply, and substrate velocity), well-aligned layers can be obtained on the area of several square centimeters, see Figure 9.[124] Zone-casting was used to align HBC-C12 and resulted in a mobility of $1 \times 10^{-2}\,cm^2\,V^{-1}\,s^{-1}$, an order of magnitude higher than oriented HBC derivatives on a PTFE layer.[125] This was consistent with Warman's findings that the photoconductivity of HBC-C12 aligned by zone-casting was 10-fold higher in the columnar alignment direction than in the perpendicular direction.[126] The optical anisotropy of an aligned HBC derivative, by the zone-casting technique, was reversibly switched on/off by changing the temperature in the region of the crystal to mesophase transition. This led to the reorientation of the molecules from a tilted to an orthogonal stacking arrangement.[127]

5.2. Zone-Melting. In the zone-melting technique, an electrically heated wire generates a narrow molten zone (0.5−2 mm wide) on the organic layer sandwiched between two pieces of glass or indium−tin oxide-coated glass, see Figure 10. When the molten zone of tetrakis-*n*-undecylporphyrin was moved slowly (3−120 μm/min) across the layer from one end of the cell to the other, a single-crystal film was produced after one pass. The steady-state short-circuit photocurrent of tetrakis-*n*-undecylporphyrin was improved by several orders of magnitude after such treatment.[128] It should be noted that the zone-melting technique also purifies the material; therefore, the improved properties may be attributed to better alignment in addition to higher purity of the material.

5.3. Langmuir−Blodgett Deposition. Alignment of amphiphilic HBC derivatives was achieved using Langmuir−Blodgett (LB) techniques.[129,130] Hexaalkylhexa-*peri*-hexabenzocoronene bearing one alkyl substituent terminated

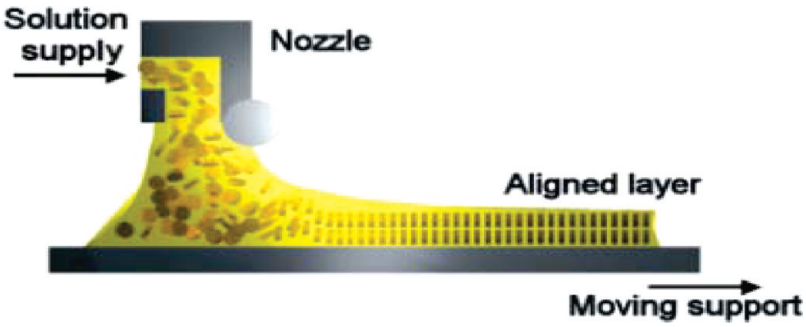

Figure 9. Schematic presentation of the zone-casting technique.[125] Pisula, W.; Menon, A.; Stepputat, M.; Lieberwirth, I.; Kolb, U.; Tracz, A.; Sirringhaus, H.; Pakula, T.; Müllen, K. "A zone-casting technique for device fabrication of field-effect transistors based on discotic hexa-*peri*-hexabenzocoronene", *Adv. Mater*. **2005**, *17*, 684−689. Copyright Wiley-VCH Verlag GmbH & Co. KGaA. Reproduced with permission.

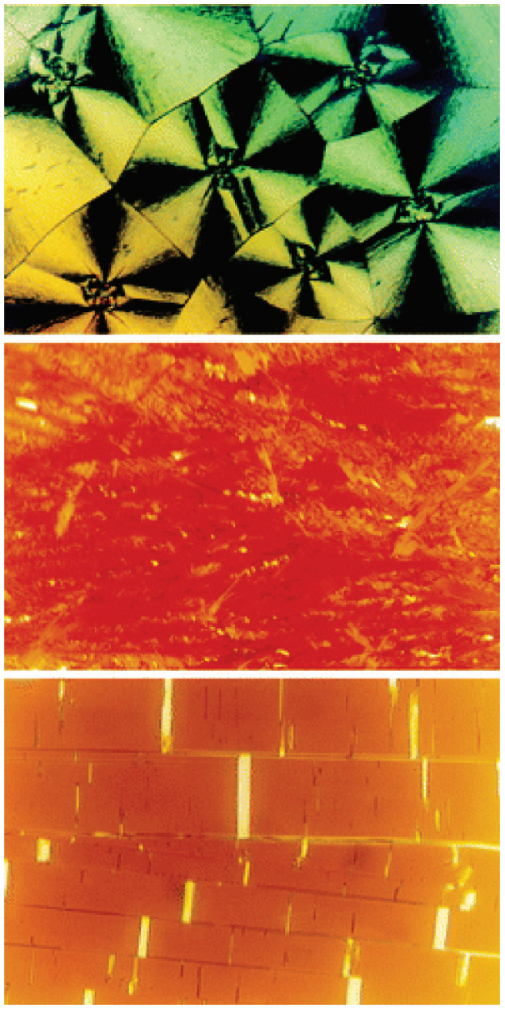

Figure 10. Micrographs of a porphyrin thin film (area of view, 0.3 mm × 0.5 mm). (top) Crystals grown by capillary filling and imaged between two crossed polarizers. (middle) Crystals first grown by capillary filling and then remelted briefly with the heating wire and quickly cooled by turning the power off. (bottom) Crystals regrown by the zone-melting technique (growth rate, 6 μm/min).[128] Reprinted with permission from ref 128. Copyright 2000 American Chemical Society.

with a carboxylic group were reported to form well-defined LB films upon growing from solution at the water−air interface.[130] The authors reported the competition of $\pi-\pi$ stacking and alkyl chain packing leading to two distinct phases.[130] Moreover, benzyl-terminated octa-substituted phthalocyanines[131] form highly ordered LB thin films of significant thermal stability while edge-on orientation was observed in LB films of DLCs formed of one/two triphenylenes linked to TNF.[132]

5.4. Solution-Casting on Preoriented Polytetrafluoroethylene (PTFE). Another tool used to align DLCs involves highly oriented polytetrafluoroethylene (PTFE). This technique was successfully applied in aligning HBC,[133] triphenylene,[134] phthalocyanine,[117] pyrene, and benzoperylene[135] derivatives into uniaxial columns along the direction of PTFE on the substrate.

Uniaxial alignment of a peritetrasubstituted phthalocyanine Pc was achieved by confining Pc in a mesh of crisscrossed nanogrooves, see Figure 11.[136] This is due to the anisotropy of boundary tension between the mesophase and the nanogrooves' walls.[136] An aligned polyimide layer surface was also used to assemble triphenylene-based DLCs.[137]

5.5. Surface Treatment. The successful alignment of DLCs by annealing is achieved when the material is stable at and slightly above the clearing temperature and when it wets the substrate in both its isotropic and DLC phase.[138] An ITO surface treatment was reported to stabilize DLC thin films, in which one treated the ITO substrate with argon plasma, annealing, and UV-ozone. This led to good wetting conditions attaining homogeneous organic thin films. Such films were obtained by heating up the DLC material above the clearing temperature and cooling down with a controlled rate to obtain large, well-aligned domains.[138] Recently, the control of planar alignment of a Pc derivative, with control of the azimuthal angle, was achieved by dewetting the compound in its isotropic phase over a substrate patterned with organothiol self-assembled monolayers on gold.[56] Alignment of DLCs can also be affected by their specific surface interactions.[120,139,140] Geerts' group reported the homeotropic alignment of a phthalocyanine derivative, attached to eight oligo(ethyleneoxy) peripheral substituents, on a hydrophilic surface whereas a planar alignment of random arrangement of column directors was observed on a hydrophobic surface.[120] The authors attributed the variation in alignment to the different interactions of the peripheral chains of the Pc molecule with the different surfaces, e.g., oligo(ethyleneoxy) chains H-bond to a hydrophilic surface causing homeotropic alignment.[120]

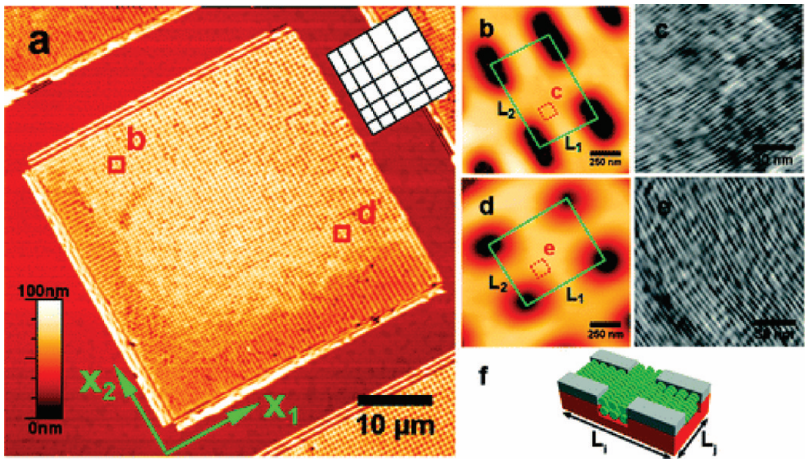

Figure 11. (a) AFM topography image of the 40 μm × 40 μm Pc network used to screen column alignment. The periods of the grooves increases progressively, as shown schematically in the inset. (b,d) AFM topographic zoom on the region marked in part a. The column alignment is observed in the corresponding AFM phase images shown in parts c and e. (f) Schematic drawing of the alignment of columns in a rectangular cell of the network.[136] Reprinted from ref 136. Copyright 2007 American Chemical Society.

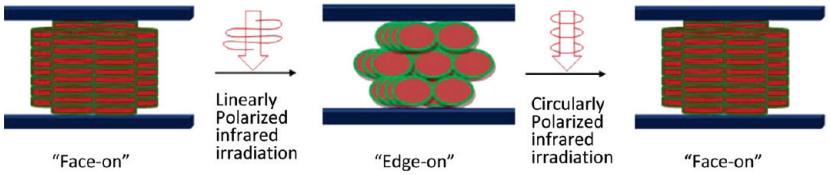

Figure 12. Schematic representation of alignment change upon circularly polarized IR irradiation.[150] Modified version of TOC from the article: Monobe, H.; Awazu, K.; Shimizu, Y. "Alignment control of a columnar liquid crystal for a uniformly homeotropic domain using circularly polarized infrared irradiation" *Adv. Mater.* **2006**, *18*, 607−610. Copyright Wiley-VCH Verlag GmbH & Co. KGaA. Reproduced with permission.

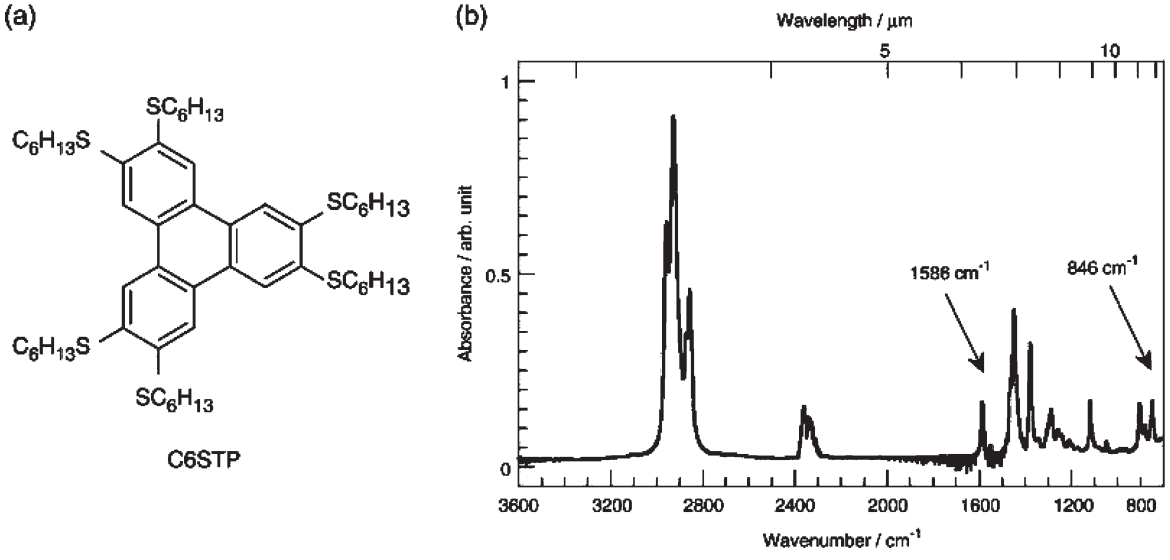

Figure 13. (a) Molecular structure of hexahexylthiotriphenylene (C6STP) and (b) its infrared spectrum of a film in H phase (66 °C).[151] Reprinted from *Thin Solid Films*, *518*, Monobe, H.; Awazu, K.; Shimizu, Y., "Alignment change of hexahexylthiotriphenylene in the helical columnar phase by infrared laser irradiation", 762−766, Copyright (2009), with permission from Elsevier.

5.6. IR Irradiation. Shimizu's group has used circularly polarized infrared irradiation to control the alignment of DLCs, see Figure 12.[141−151] The vibrational mode of a selected chemical bond in a mesogen is excited using polarized infrared irradiation from a free electron laser leading to a change of DLC alignment.[146] The selected combination of the polarization direction of the incident photon as well as that of the transition dipole moment for the vibrational excitation allows achieving the molecular alignment. Such alignment can only be obtained with the higher-ordered DLC phase, Col_h mesophase, owing to its high viscocity.[146] The polarized infrared light irradiation of the C−C stretching absorption band of hexahexylthiotriphenylene (C6STP) (1 586 cm^{-1}) led to a uniform and anisotropic alignment change of domains, see Figures 13 and 14.[151]

5.7. Magnetic. Lee et al. reported the first magnetic uniaxial alignment of the columnar structures of discotic

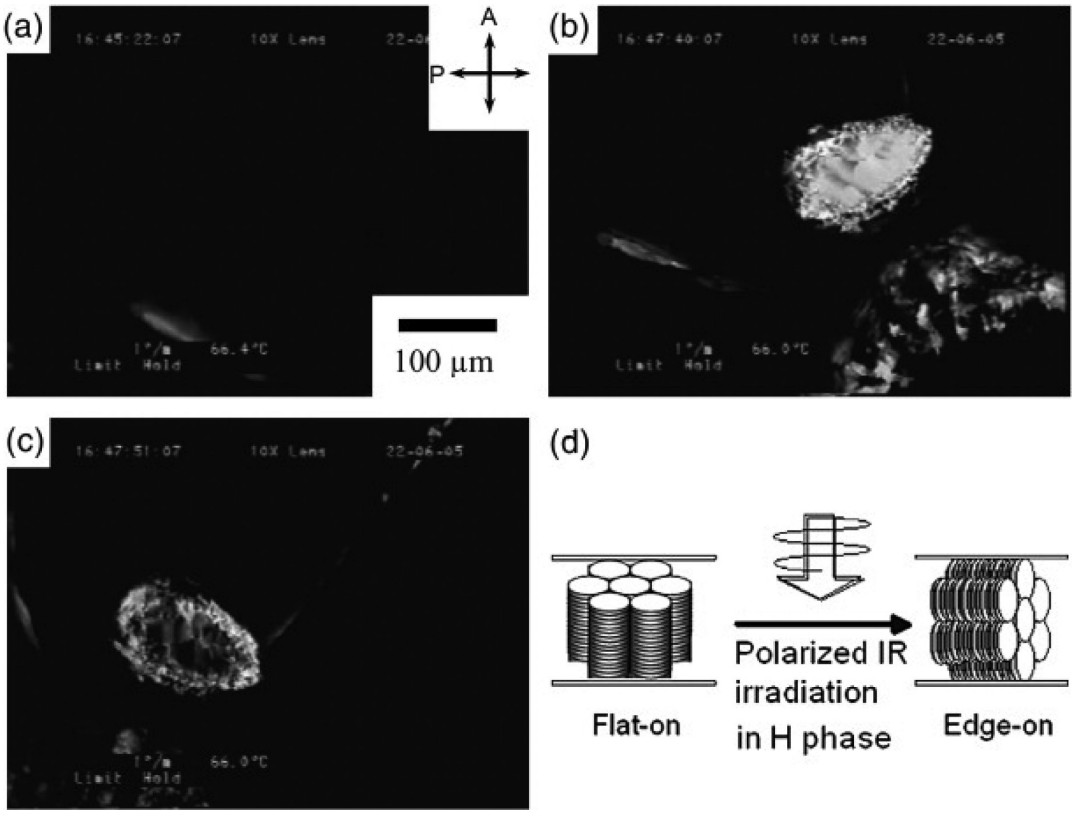

Figure 14. Microscopic textures observed for a C6STP film in H phase at 66 °C cooled from I.L. followed by Col_h (a) before infrared irradiation (homeotropic alignment), (b) after irradiation with 6.30 μm infrared FEL and (c) after rotation of the sample on the stage by 45° counterclockwise. (d) A schematic representation of the alignment change of columns in H phase of C6STP with infrared laser irradiation.[151] Reprinted from *Thin Solid Films*, *518*, Monobe, H.; Awazu, K.; Shimizu, Y., "Alignment change of hexahexylthiotriphenylene in the helical columnar phase by infrared laser irradiation", 762−766, Copyright (2009), with permission from Elsevier.

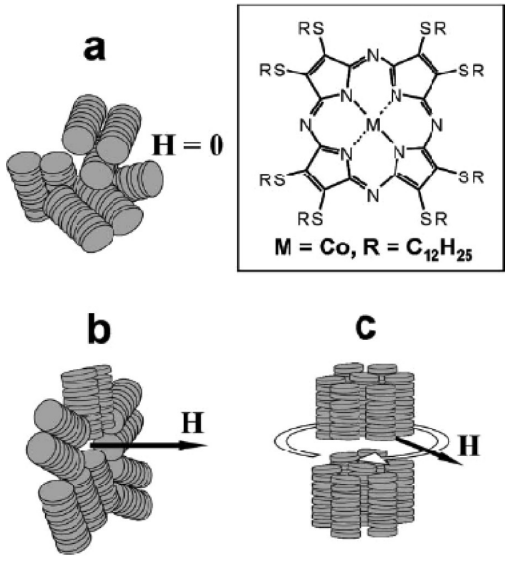

Figure 15. Uniaxial alignment concept using a rotating magnetic field.[152] Lee, J.-H.; Choi, S.-M.; Pate, B. D.; Chisholm, M. H.; Han, Y.-S. "Magnetic uniaxial alignment of the columnar superstructure of discotic metallomesogens over the centimetre length scale", *J. Mater. Chem.* **2006**, *16*, 2785−2791. Reproduced by permission of the Royal Society of Chemistry.

metallomesogens, cobalt octa(*n*-dodecylthio)porphyrazine (CoS12), see Figure 15, over a centimeter length scale.[152,153] Because the DLC aromatic core possesses a diamagnetic interaction with an external magnetic field, uniaxial alignment can be achieved by cooling a constantly spinning sample from the isotropic phase to the liquid crystalline phase in the presence of a static applied magnetic field.[152] Edge-on alignment in CoS12 DLC was achieved using an external magnetic field (∼1.0 T) and a substrate functionalized with octadecyltrichlorosilane (OTS), which increases the affinity of the substrate to the alkyl side chains.[154] The magnetic alignment of HBC derivative resulted in a charge-carrier mobility up to 10^{-3} cm^2 V^{-1} cm^{-1} in an FET device.[155]

5.8. Use of a Sacrificial Layer. Geerts' group reported the use of a sacrificial polymer layer for confinement of an alkoxy phthalocyanine DLC to achieve homeotropic alignment.[156] After spin coating the Pc on the substrate, the sacrificial polymer is spin-cast. Thermal annealing followed by cooling to room temperature induces the homeotropic alignment. The sacrificial polymer is then washed carefully with methanol, see Figure 16.[156]

5.9. Blends. The morphological studies of blends of different mesogenic binary discotic systems leading to spontaneous alignment without application of external stimuli are recently reported.[157−161] The columnar phase of blends of more than 40% of disk-shaped electron-donor phthalocyanine and the lath-shaped perylenetetracarboxidiimide derivatives was shown to be more ordered with the increase of phase stability of 100 °C in comparison to pure Pc.[159] The authors proposed the random insertion of lathlike molecules inside molecules of disks in

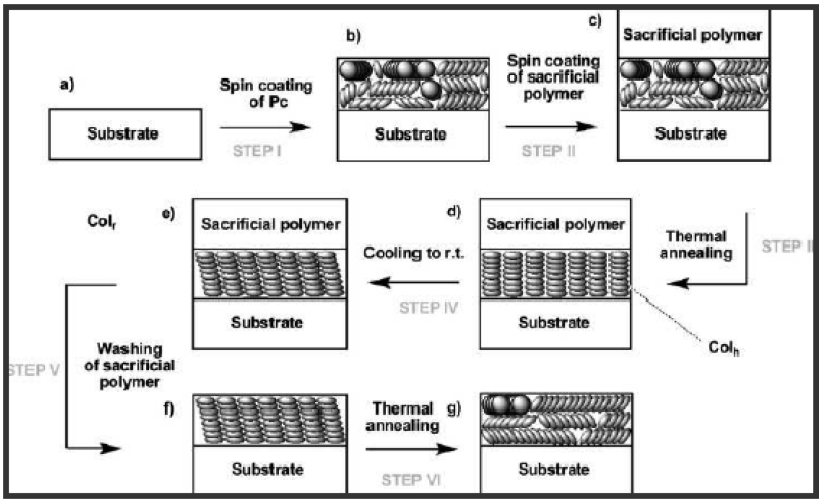

Figure 16. Fabrication process of homeotropically aligned films of the phthalocyanine derivative. The last step serves only to demonstrate the function of the sacrificial layer.[156] Reprinted from ref 156. Copyright 2009 American Chemical Society.

the columnar phase leading to self-aligned homeotropic alignment between two electrodes.[159] Geerts' group demonstrated that homeotropic alignment in blends of two metal-free Pc mesogens is only possible when one of the compounds exhibits a Col$_h$ phase.[158] Complementary polytopic interaction (CPI),[162] which is defined as the sum total of a large number of atom-by atom van der Waals interactions between a discotic mesogen and a larger core polyaromatic compound,[163] in a 1:1 mixture of 2,3,6,7,10,11-hexakis(hexyloxy)triphenylene (has Col$_h$ phase between 70 and 100 °C) and hexakis(4-nonylphenyl)dipyrazino-[2,3-*f*:2′3′-*h*]quinoxaline (has two crystal forms that melt at 71 and 81 °C) resulted in a Col$_h$ phase with a clearing temperature of 240 °C.[9] Recently, C60-discotic dyads forming mesophases were reported.[164,165] C60, anchored to two triphenylene moieties via dodecyloxy side chains, produced a CPI columnar phase when mixed with dipyrazino[2,3-*f*:2′,3′-*h*]quinoxaline derivative.[164] The authors proposed the clustering of fullerenes around one of the seven columns forming this Col$_h$ phase.[164] Monte Carlo simulations of the phase behavior and molecular organization of the triphenylene-C60-triphenylene mesogenic unit showed mesomorphism with isotropic, nematic, and columnar phases wherein the fullerenes are closely packed.[166]

5.10. Influence of Electric Field on Alignment. The response of DLC materials to an applied electric field was also investigated.[167−175] The design of a ferroelectric columnar DLC requires the stabilization of one-directional stacking of molecules in the column and the reduction of the intercolumnar dipole−dipole interaction to reduce the repulsive interaction between the columns in the ferroelectric arrangement.[170] Kishikawa's group reported the Col$_h$ mesophases of *N*,*N*′-bis(3,4,5-trialkoxyphenyl)-ureas (R = *n*-$C_{12}H_{25}$ and *n*-$C_{16}H_{33}$), in which the urea molecules are stacked in one direction in each column with strong H-bonding, to exhibit a sharp peak of spontaneous polarization in response to an applied triangular electric field (0.1−18 Hz), see Figure 17.[170] Homeotropic

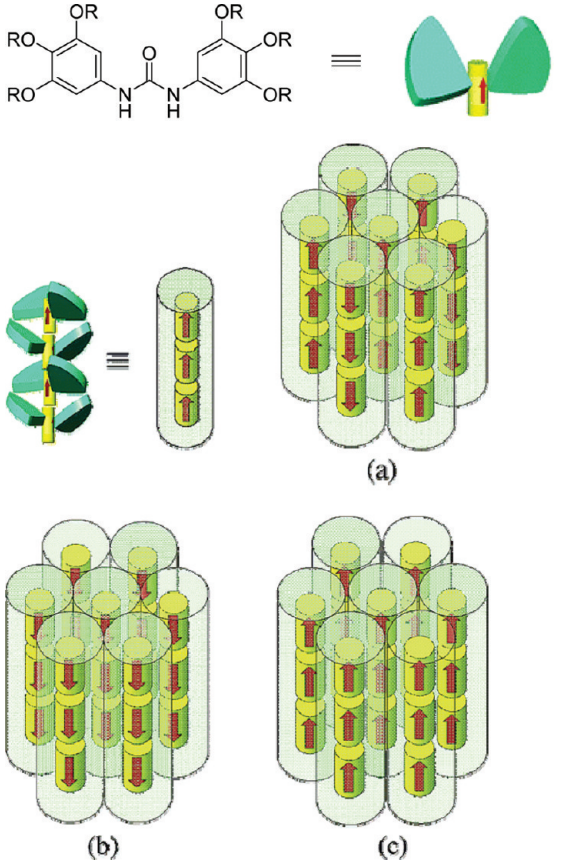

Figure 17. Schematic representation of columnar DLC columns of *N*,*N*′-bis(3,4,5-trialkoxyphenyl)ureas (R = C_nH_{2n+1}) in the switching experiment. (a) Columns at 0 V; (b and c) columns in an applied field.[170] Reprinted from ref 170. Copyright 2005 American Chemical Society.

alignment of DLC materials was also achieved upon the application of an electric field.[173,174]

5.11. Others. Dewetting of columnar DLCs of triphenylene and phthalocyanine derivatives on chemically patterned surfaces resulted in planar alignment.[172,175] Bock's group reported the competition of homeotropic and planar alignment in DLCs which can be controlled by the film thickness and cooling rate.[176,177] The induced

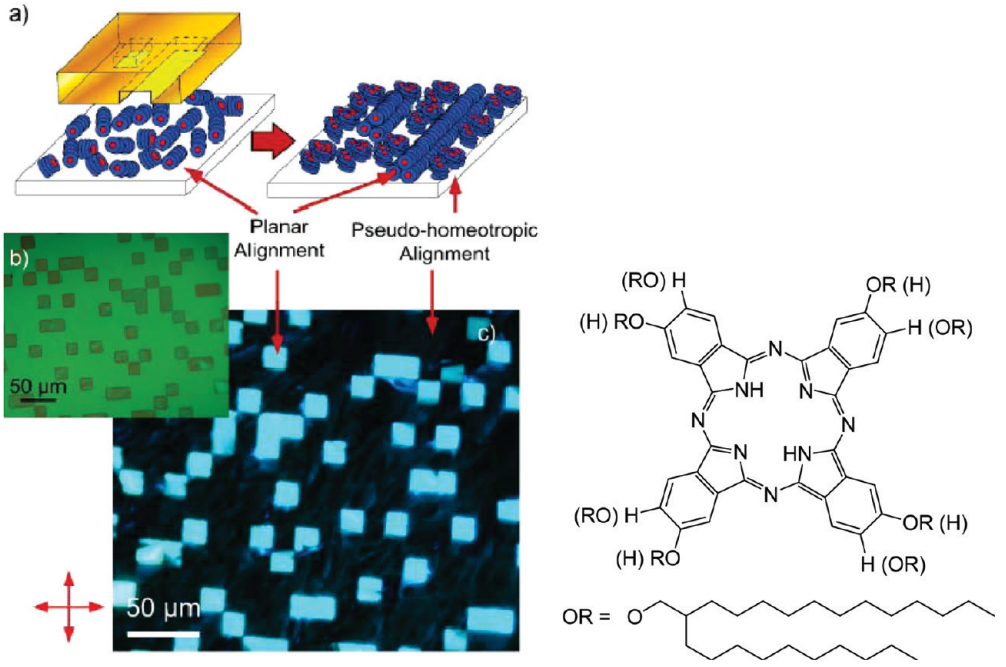

Figure 18. LCW induces a spatially controlled columns orientation in continuous thin films. a) Scheme of LCW applied on isotropic (fluid) phase. b) Optical microscopy images in bright field of the stamp and c) with cross polars of the patterned Pc film.[185] Cavallini, M.; Calo, A.; Stoliar, P.; Kengne, J. C.; Martins, S.; Matacotta, F. C.; Quist, F.; Gbabode, G.; Dumont, N.; Geerts, Y. H.; Biscarini, F. "Lithographic Alignment of Discotic Liquid Crystals: A New Time-Temperature Integrating Framework", *Adv. Mater.* **2009**, *21*, 4688−4691. Copyright Wiley-VCH Verlag GmbH & Co. KGaA. Reproduced with permission.

birefringence observed between crossed polarizers is indicative of planar alignment whereas the absence of birefringence is typical of hometropic alignment since the direction of light propagation is parallel to the optical axis of the liquid crystal.[176]

Substitution of triphenylene with fluoroalkylated groups further resulted in a greater tendency for homeotropic alignment.[178] The presence of fluoroalkylated chain spacer, linked to the pentakis(phenylethynyl)-phenoxy core, was also reported to stabilize the nematic phase of this DLC.[179] The gelation of hexahexyloxytriphenylene has resulted in a 3-fold increase of its hole mobility up to 1.2×10^{-3} cm^2 V^{-1} s^{-1},[180] which was attributed to the suppression of fluctuation of the triphenylene molecules and increase of the molecular order in the gelated discotics.[180,181]

Triphenylene DLCs were also photoaligned on the surface of thin films of photoirradiated azobenzene-containing polymer[182] and photo-cross-linkable polymer with cinnamoyl side groups.[183] When an azobenzene-containing polymer film was exposed to oblique nonpolarized light, photoisomerization and reorientation of azobenzene was achieved. This resulted in tilted DLC orientation forming a columnar nematic phase. However, the exposure of the film to linearly polarized light led to the homeotropic alignment of the triphenylene DLC.[184]

Recently, the lithographic controlled wetting (LCW) technique was exploited to align the metal-free mesogenic phthalocyanine DLC, see Figure 18.[185] The authors reported the films to be patterned with no effect of aging at ambient temperature.[185] LCW is an unconventional lithographic method that is capable of forming a patterned nanostructure from a liquid layer.[186,187]

Moreover, Geerts' group reported the substrate-independent nature of the homeotropic alignment of mesogenic phthalocyanine.[188] The authors demonstrated homeotropic alignment of Pc even with substrates of different surface roughness, surface correlation lengths, and surface energies.[188] They also showed that it is the confinement induced by solid substrates, rather than the nature of substrates, that controls the homeotropic alignment.[188]

Finally, atomic force microscopy (AFM)[159,189−197] and scanning tunneling microscopy (STM)[198−203] were largely used to characterize the hierarchical self-assembly of DLCs on conductive substrates. STM allows the study of the dynamics of monolayers in addition to the depiction of molecular ordering.[200] Piot et al. showed the spontaneous hierarchical self-assembly of edge-on nanocolumnar stacks of HBC-C12 at the liquid−solid interface on highly oriented pyrolitic graphite (HOPG).[198] The authors attributed the complex 3D supramolecular multilayered architectures (HOPG/face-on/edge-on/edge-on) and (HOPG/face-on/edge-on/face-on) to the strong tendency of HBC-C12 to aggregate in π-stacks or mesophases.[198]

6. Theoretical Calculations

Brédas and co-workers reported a seminal quantum-chemical study correlating structures and properties of DLCs and the subsequent effect on their charge-transport properties.[204,205] The estimation of phonon-assisted hopping between the discoid mesogens in DLCs is based on the idea that electrons (or holes) are localized on the discs and they hop from one disk to another along the stacking axis. Two main parameters govern charge transport in DLCs at the molecular scale: the reorganization energy

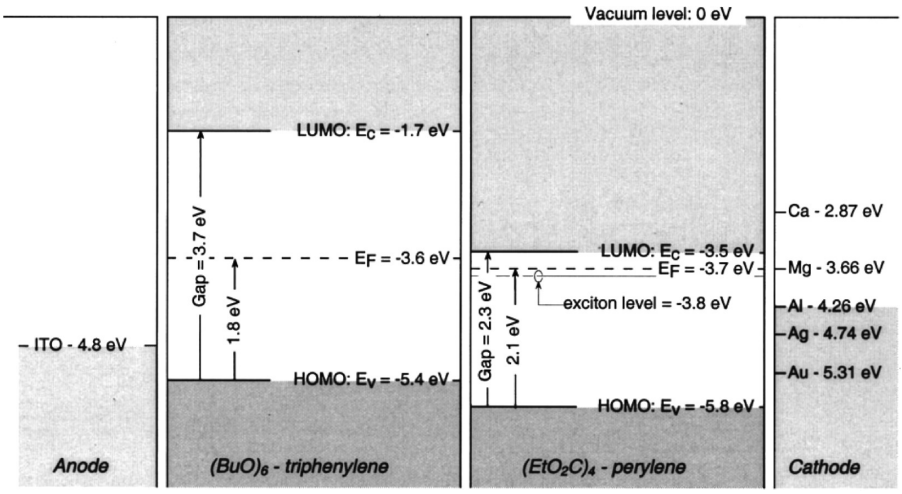

Figure 19. Schematic band diagram of OLED made of triphenylene and perylene.[209] Reprinted with permission from Seguy, I.; Jolinat, P.; Destruel, P.; Farenc, J.; Mamy, R.; Bock, H.; Ip, J.; Nguyen, T. P. *J. Appl. Phys.* **2001**, *89*, 5442−5448. Copyright 2001, American Institute of Physics.

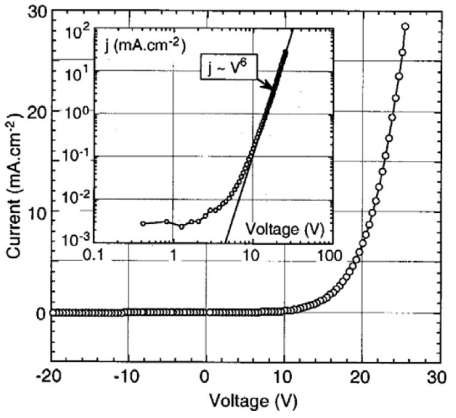

Figure 20. Current density-voltage characteristics of the EL device.[209] Reprinted with permission from Seguy, I.; Jolinat, P.; Destruel, P.; Farenc, J.; Mamy, R.; Bock, H.; Ip, J.; Nguyen, T. P. *J. Appl. Phys.* **2001**, *89*, 5442−5448. Copyright 2001, American Institute of Physics.

(λ) and the intermolecular transfer integral (t). The reorganization energy is the sum of the internal reorganization energy, which is related to the geometric differences between neutral and charged species and that of the surrounding medium. In a dimer of two neutral molecules, the strength of electronic coupling, t, between them can be estimated as half the electronic splitting, respectively, of the HOMO and LUMO levels for holes and electrons. To achieve high charge-carrier mobilities in DLCs, small values of λ and large values of t are desired.[205] The authors reported the magnitude of the transfer integrals in model dimers to be strongly governed by the rotational angle between two adjacent π-stacked molecules and hence the increase in the discoid size would not necessarily result in higher charge-carrier mobility. Furthermore, the authors demonstrated that the shape of the molecules does not influence the calculated electronic coupling as much as that of the character of the electronic wave function.[205] Electron-transport DLCs should, therefore, have a small value of λ, large value of t, and an electron deficient core to facilitate the electron injection/collection. Hexakis(alkylsulfanyl)hexaazatrinapthylene HATNA-$[SR]_6$ mesogens were designed with the aforementioned requirements to act as potential electron-transport materials.[49] PR-TRMC mobilities of HATNA-$[SR]_6$ showed the strong dependence on the nature of the side chains with a 0.26 $cm^2\ V^{-1}\ s^{-1}$ for HATNA-$[SC_{10}H_{21}]_6$ at 180 °C.[49] The charge-transport parameters of HBC derivatives were estimated at different temperatures using a simplified INDO method[206] and a combination of quantum chemical calculations, molecular dynamics, and kinetic Monte Carlo simulations.[207] Molecular dynamic simulations of tetraalkoxy-subsituted metal-free phthalocyanines show the association between charge transport mechanism and the dynamics of mesophases.[208] The hole mobility is 2 orders of magnitude higher (10^{-1} vs $10^{-3}\ cm^2\ V^{-1}\ s^{-1}$) when accounting for the rotational and translational dynamics (dynamic vs static approach).[208]

7. Optoelectronic Devices

A red organic light emitting device made from the electron-rich 2,3,6,7,10,11-hexabutoxytriphenylene and the electron-poor fluorescent tetraethylperylene-3,4,9,10-tetracarboxylate, both of which show DLC phases at high temperature, was recently reported.[209] The device structure was ITO/triphenylene hexaether/perylene tetraester/aluminum. Electrons are injected from the aluminum cathode into the perylene layer, whereas holes are injected from the ITO anode, see Figure 19. The charge recombination occurs in the perylene layer near the heterojunction, and the emission leads to red light with λ_{max} = 615 nm. The current density was reported to reach as high as 28 mA cm^{-1} at 26 V. At 28 V, a maximum luminance of 45 cdm^{-1} was recorded with the light turning on at 16 V, see Figure 20.[209]

Schmidt-Mende et al. reported the first use of DLC materials in an OPV device.[210] The authors used the self-assembly properties of hexabenzocoronene DLC derivative and perylene dimide to fabricate an OPV device with a maximum external quantum efficiency of more than 34% near 490 nm and a power efficiency up to 2%.[210] The authors attributed the high efficiency to photoinduced

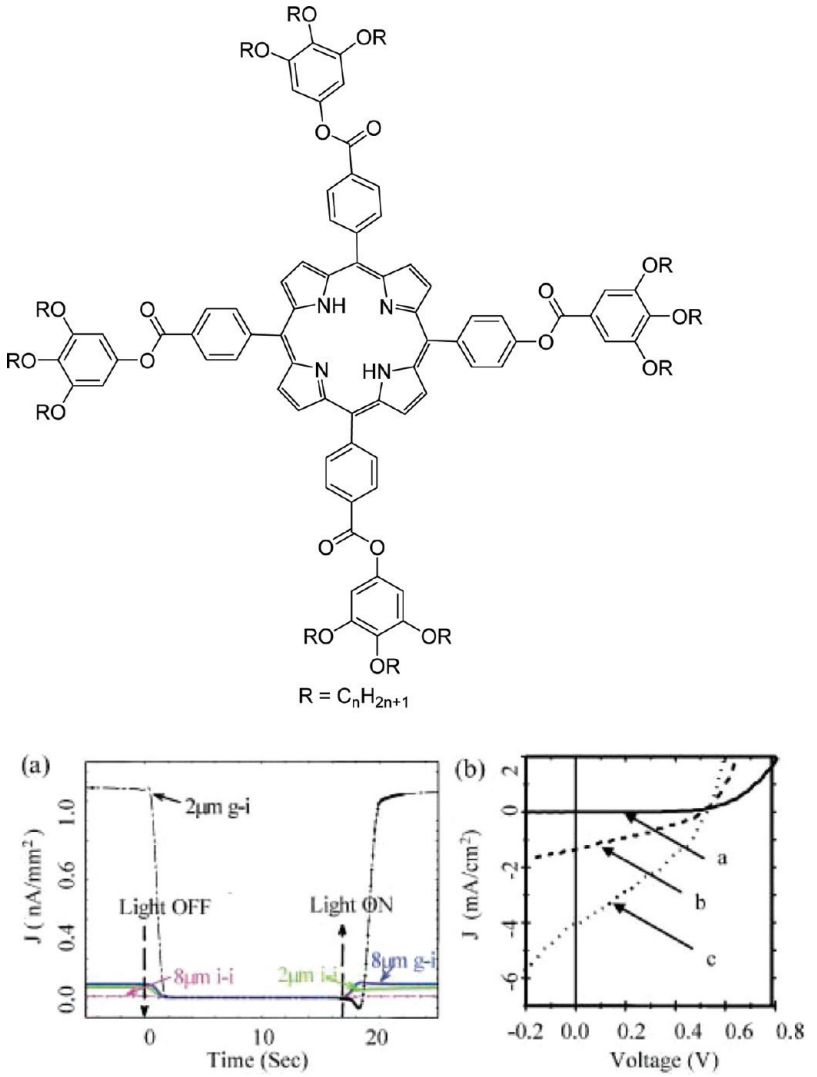

Figure 21. *J*−*V* characteristics of the bulk heterojunction cell.[211] Li, L.; Kang, S.-W.; Harden, J.; Sun, Q.; Zhou, X.; Dai, L.; Jakli, A.; Kumar, S.; Li, Q. *Liq. Cryst.* **2008**, *35*, 233−239, reprinted by permission of the publisher (Taylor & Francis Group, http://www.informaworld.com).

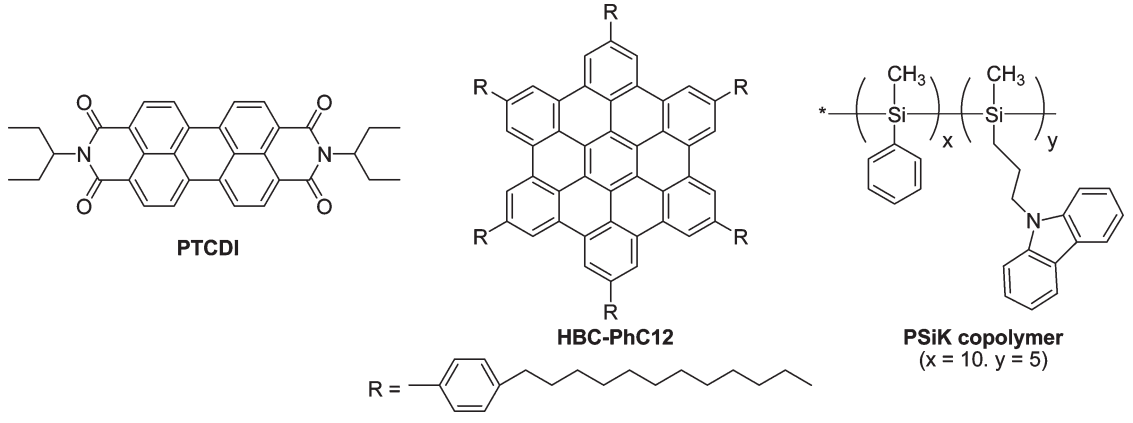

Figure 22. Structures used in Müllen's PV device.[212]

charge transfer between the hexabenzocoronene and perylene along the π-system.[210] The investigation of a bulk heterojunction PV cell formed from a 1:1 (w/w) blend of a DLC porphyrin electron donor (see Figure 21, R = $C_{12}H_{25}$) and the C_{60} derivative (PCBM) as an electron acceptor, where the ITO anode was coated with a conducting polymer poly(3,4-ethylenedioxythiophene) (PEDOT) and the cathode was Ca/Al, showed a power conversion efficiency (PCE) of 0.222%.[211] The PCE increased to 0.712% upon postannealing treatment leading to a better alignment of the porphyrin.[211]

Moreover, Müllen's group reported preparation of a PV device by spin-coating a 40:60 mixture of HBC-PhC12−PTCDI (see Figure 22), dissolved in chloroform,

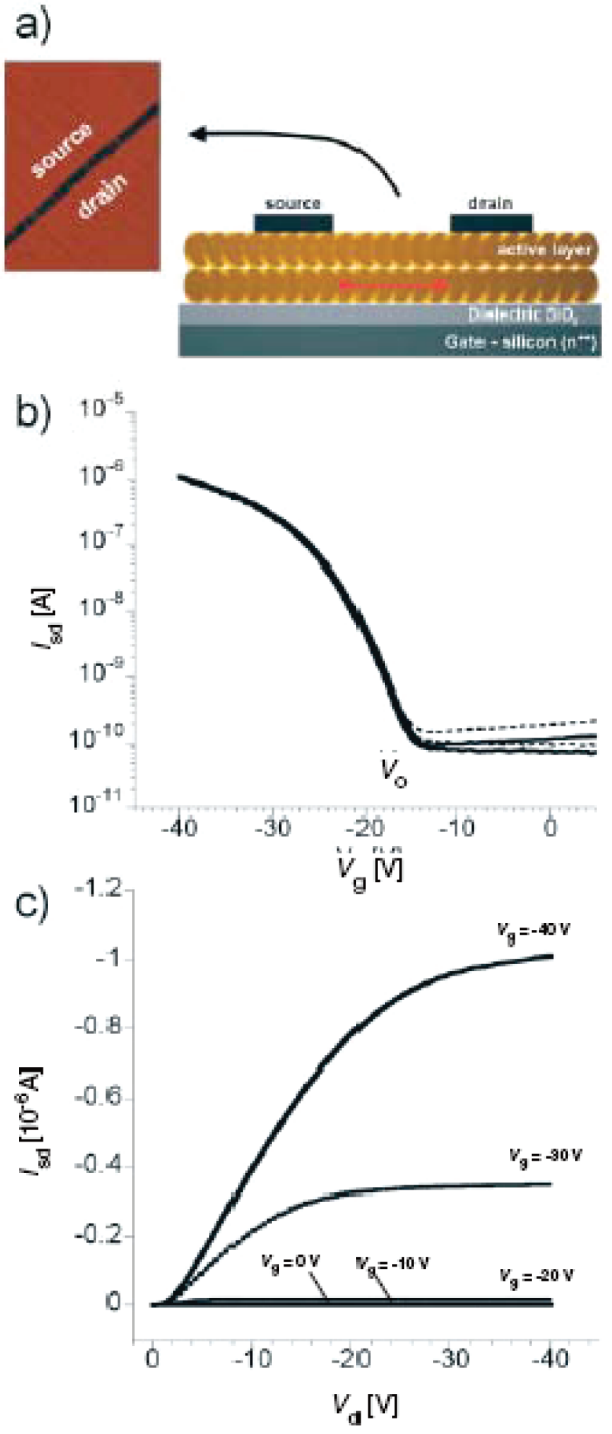

Figure 23. a) Schematic presentation of the top-contact device configuration (channel length L = 25 mm, width W = 1.6 mm, and depth d = 200 nm) onto a 20 nm thick zone-cast HBC-C_{12} aligned film. A 200 nm SiO_2 dielectric gate and an n-doped silicon substrate as a gate electrode were used in this device configuration. b) Transfer characteristic (gate voltage Vg = −40 V). c) Current-voltage (I–V) output characteristics. Both dependences are measured along the columnar alignment. V_d: drain voltage; I_{sd}: source-drain current.[125] Pisula, W.; Menon, A.; Stepputat, M.; Lieberwirth, I.; Kolb, U.; Tracz, A.; Sirringhaus, H.; Pakula, T.; Müllen, K. "A zone-casting technique for device fabrication of field-effect transistors based on discotic hexa-peri-hexabenzocoronene", *Adv. Mater.* **2005**, *17*, 684−689. Copyright Wiley-VCH Verlag GmbH & Co. KGaA. Reproduced with permission.

on ITO-coated glass substrate and covering it with a 20 nm thin film of poly(ethylenedioxythiophene) doped

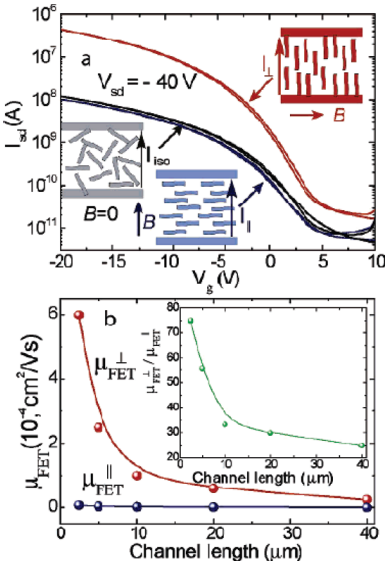

Figure 24. Electrical performance of HBC-PhC_{12}-based FET (L = 10 m; W = 10 mm). (a) Transfer characteristics for oriented HBC layers ($I_{\perp}$, red line), parallel ($I_{||}$, blue line) to the magnetic direction and active HBC layers without the application of magnetic field (I_{iso}, black line). Insets show the direction of the field direction B and HBC-PhC_{12}. (B) Dependence of field- effect mobility on the channel length.[155] Reprinted from ref 155. Copyright 2005 American Chemical Society.

with polystyrene sulfonic acid (PEDOT-PSS).[212] The performance of the photodiode was shown to be dependent on film morphology wherein the highest short circuit current JSC density was obtained with 1 wt % addition of the photoconducting copolymer PSiK.[212]

The control of morphology of a PV device formed of blends of electron-acceptor perylene tetracarboxdiimide (EPPTC) and electron-donor HBC improved the photovoltaic response with an external quantum efficiency up to 29.5% at 460 nm and an open circuit voltage of 0.70 V.[213] This was achieved by controlling the annealing of the HBC−EPPTC blend deposited on an elastomeric stamp of low-surface roughness.[213] The formation of "interpenetrating networks" between the electron-transport and hole-transport materials is crucial in preparing blend devices.[214]

Furthermore, an OPV device formed of the ITO/triphenylene derivative/perylene/Al structure generated an external quantum efficiency of 3%, which was attributed to high exciton-diffusion lengths, high absorption coefficients, and optimized organic/inorganic interface.[215]

An OFET device was constructed using aligned HBC-C_{12} via the zone-casting technique with top contacts of 25 μm channel length with saturation mobility up to 5 × 10^{-3} cm^2 V^{-1} s^{-1}, see Figure 23.[125] The on−off ratio was 10^4 and the turn-on voltage was ∼15 V.[125] Moreover, a solution processed OFET device made of magnetically aligned HBC-PhC_{12} was fabricated with charge-carrier mobility of $10^{-3}$$cm^2$ V^{-1} cm^{-1} along the perpendicular direction to the applied magnetic field, 10-fold higher than in the parallel direction or in the absence of magnetic field. The on−off ratio was 10^4 and the turn-on voltage was ∼5 V, see Figure 24.[155] Recently, bottom gold contact, bottom-gate ambipolar OFETs were fabricated by drop casting tetracarboxdiimide (SWQDI), see Figure 25,

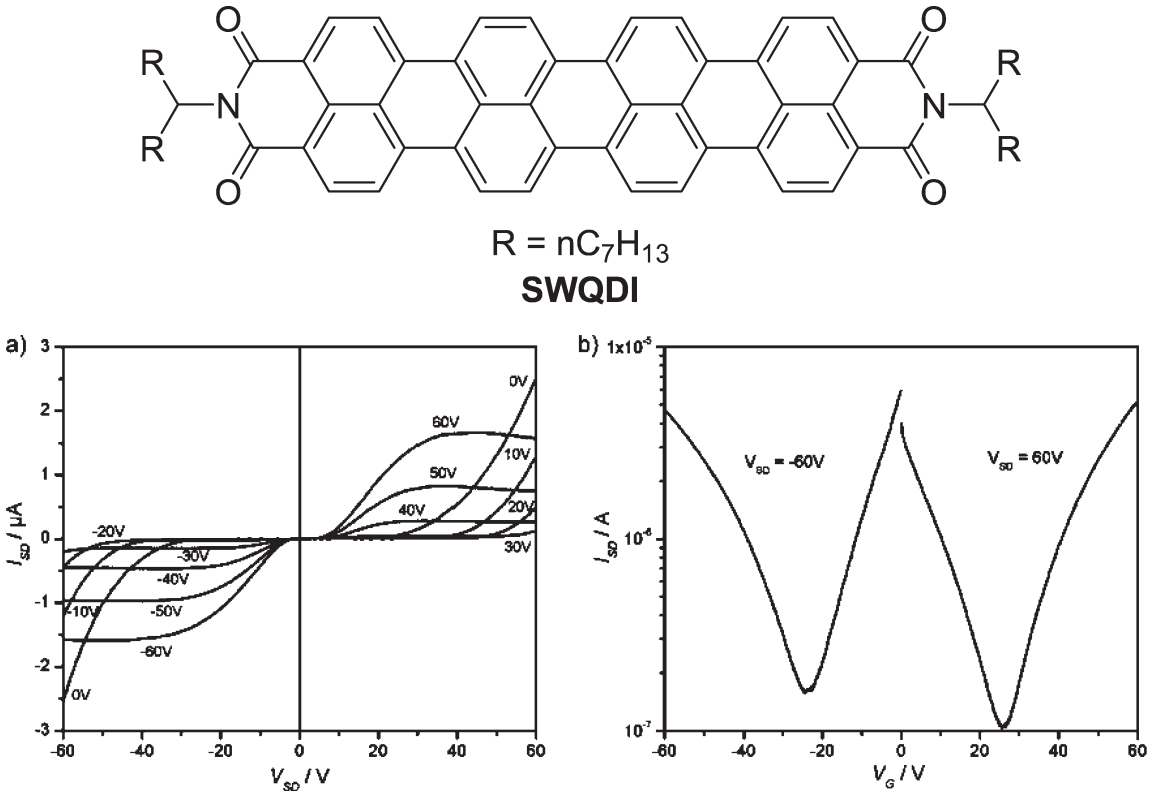

Figure 25. a) Output and b) transfer characteristics (at V_{SD} = 60 V) of an ambipolar SWQDI FET.[216] Tsao, H. N.; Pisula, W.; Liu, Z.; Osikowicz, W.; Salaneck, W. R.; Müllen, K. "From ambi- to unipolar behavior in discotic dye field-effect transistors", *Adv. Mater.* **2008**, *20*, 2715−2719. Copyright Wiley-VCH Verlag GmbH & Co. KGaA. Reproduced with permission.

on hexamethyldisilazane (HMDS)-treated SiO_2 substrates.[216] The hole mobility was 1×10^{-3} cm^2 V^{-1} s^{-1} while the electron mobility was 1.5×10^{-3} cm^2 V^{-1} s^{-1}.[216] OFETs using *N*,*N*-dialkyl-3,4,9,10-perylene tetracarboxylic diimides were also reported with an electron mobility up to 1.7 cm^2 V^{-1} s^{-1} (for R = octyl) with an on−off current ratio of 10^7.[217] Moreover, solution-processed OFETs were fabricated using NIR-absorbing tetraoctyl-substituted vanadyl phthalocyanine, which exhibits a columnar rectangular mesophase, forming edge-on aligned molecules in a spin-cast film with mobility up to 0.017 cm^2 V^{-1} s^{-1}.[218] OFETs based on a triphenylene derivative were also reported.[219] Nuckolls' group reported the fabrication of stable high-performance photosensitive OFETs, produced from self-assembled HBC derivatives using single-walled carbon nanotubes (SWNTs) as point contacts, with resistance up to 8.99×10^9 Ω.[220] Furthermore, Fiji Photo Film Company showed the use of hybrid aligned DLCs to be effective in increasing the view of angle of thin-film transistor liquid-crystal displays.[221−223]

8. Conclusions and Future Outlook

Despite numerous reports on the synthesis and characterization of DLCs, the exploitation of DLCs in opto-electronic devices is still in its infancy. Only very few discotics have been reported in electronic devices in which the obtained results were truly encouraging. Though reports of DLCs with potentially attractive properties are extensive, optimization of their properties is far from complete. The use of a suitable processing technique to align DLCs in the optimized arrangement is fundamental to achieve an efficient functioning device. It is conceivable that DLCs will have an excellent impact in opto-electronics in the near future.

Acknowledgment. The author would like to thank the thorough review of the four reviewers of this manuscript. The author would like also to thank Prof. Douglas C. Neckers, Prof. Brigitte Wex, and Dr. Stephen Barlow for many suggestions and for proofreading this manuscript. The work of the author described in this manuscript was supported by the Petroleum Research Fund (PRF) of the American Chemical Society (Grant No. 47343-B10), the Masri Institute of Energy and Natural Resources, the Royal Society of Chemistry, the University Research Board (URB) of the American University of Beirut, and the Lebanese National Council for Scientific Research (CNRS). The author is grateful for this support.

References

(1) Chandrasekhar, S.; Sadashiva, B. K.; Suresh, K. A. *Pramana* **1977**, *9*, 471–480.
(2) Kumar, S. *Liq. Cryst.* **2004**, *31*, 1037–1059.
(3) Kumar, S. *Chem. Soc. Rev.* **2006**, *35*, 83–109.
(4) Barbera, J.; Rakitin, O. A.; Ros, M. B.; Torroba, T. *Angew. Chem., Int. Ed.* **1998**, *37*, 296–299.
(5) Höger, S. *Chem.—Eur. J.* **2004**, *10*, 1320–1329.
(6) Ionov, R.; Angelova, A. *J. Phys. Chem. B* **1995**, *99*, 17593–17605.
(7) Bushby, R. J.; Lozman, O. R. *Curr. Opin. Colloid Interface Sci.* **2002**, *7*, 343–354.
(8) Praefcke, K.; Eckert, A. *Mol. Cryst. Liq. Cryst.* **2003**, *396*, 265–299.
(9) Boden, N.; Bushby, R. J.; Lozman, O. R. *Mol. Cryst. Liq. Cryst.* **2003**, *400*, 105–113.

(10) Kumar, S. *Curr. Sci.* **2002**, *82*, 256–257.
(11) Kumar, S. *Pramana* **2003**, *61*, 199–203.
(12) Kumar, S. *Liq. Cryst.* **2005**, *32*, 1089–1113.
(13) Laschat, S.; Baro, A.; Steinke, N.; Giesselmann, F.; Haegele, C.; Scalia, G.; Judele, R.; Kapatsina, E.; Sauer, S.; Schreivogel, A.; Tosoni, M. *Angew. Chem., Int. Ed.* **2007**, *46*, 4832–4887.
(14) Sergeyev, S.; Pisula, W.; Geerts, Y. H. *Chem. Soc. Rev.* **2007**, *36*, 1902–1929.
(15) Pisula, W.; Zorn, M.; Chang, J. Y.; Müllen, K.; Zentel, R. *Macromol. Rapid Commun.* **2009**, *30*, 1179–1202.
(16) Nelson, J.; Kwiatkowski, J. J.; Kirkpatrick, J.; Frost, J. M. *Acc. Chem. Res.* **2009**, *42*, 1768–1778.
(17) Feng, X.; Pisula, W.; Müllen, K. *Pure Appl. Chem.* **2009**, *81*, 2203–2224.
(18) Bisoyi, H. K.; Kumar, S. *Chem. Soc. Rev.* **2010**, *39*, 264–285.
(19) Kumar, S. *Liq. Cryst.* **2009**, *36*, 607–638.
(20) Caprion, D.; Bellier-Castella, L.; Ryckaert, J. P. *Phys. Rev. E: Stat., Nonlinear, Soft Matter Phys.* **2003**, *67*, 041703/1−041703/8.
(21) Zharnikova, N.; Usol'tseva, N.; Kudrik, E.; Thelakkat, M. *J. Mater. Chem.* **2009**, *19*, 3161–3167.
(22) Tschierske, C. *J. Mater. Chem.* **1998**, *8*, 1485–1508.
(23) Cornil, J.; Beljonne, D.; Calbert, J.-P.; Brédas, J.-L. *Adv. Mater.* **2001**, *13*, 1053–1067.
(24) Crispin, X.; Cornil, J.; Friedlein, R.; Okudaira, K. K.; Lemaur, V.; Crispin, A.; Kestemont, G.; Lehmann, M.; Fahlman, M.; Lazzaroni, R.; Geerts, Y.; Wendin, G.; Ueno, N.; Brédas, J.-L.; Salaneck, W. R. *J. Am. Chem. Soc.* **2004**, *126*, 11889–11899.
(25) Kim, Y. H.; Yoon, D. K.; Jung, H.-T. *J. Mater. Chem.* **2009**, *19*, 9091–9102.
(26) Hennrich, G.; Cavero, E.; Barbera, J.; Gomez-Lor, B.; Hanes, R. E.; Talarico, M.; Golemme, A.; Serrano, J. L. *Chem. Mater.* **2007**, *19*, 6068–6070.
(27) Jeong, M. J.; Park, J. H.; Lee, C.; Chang, J. Y. *Org. Lett.* **2006**, *8*, 2221–2224.
(28) Zhang, Y.-D.; Jespersen, K. G.; Kempe, M.; Kornfield, J. A.; Barlow, S.; Kippelen, B.; Marder, S. R. *Langmuir* **2003**, *19*, 6534–6536.
(29) Grafe, A.; Janietz, D.; Frese, T.; Wendorff, J. H. *Chem. Mater.* **2005**, *17*, 4979–4984.
(30) Meier, H.; Lehmann, M.; Holst, H. C.; Schwoppe, D. *Tetrahedron* **2004**, *60*, 6881–6888.
(31) Attias, A.-J.; Cavalli, C.; Donnio, B.; Guillon, D.; Hapiot, P.; Malthete, J. *Mol. Cryst. Liq. Cryst.* **2004**, *415*, 169–177.
(32) Pieterse, K.; Lauritsen, A.; Schenning, A. P. H. J.; Vekemans, J. A. J. M.; Meijer, E. W. *Chem.—Eur. J.* **2003**, *9*, 5597–5604.
(33) Ichihara, M.; Suzuki, H.; Mohr, B.; Ohta, K. *Liq. Cryst.* **2007**, *34*, 401–410.
(34) Roussel, O.; Kestemont, G.; Tant, J.; de Halleux, V.; Aspe, R. G.; Levin, J.; Remacle, A.; Gearba, I. R.; Ivanov, D.; Lehmann, M.; Geerts, Y. *Mol. Cryst. Liq. Cryst.* **2003**, *396*, 35–39.
(35) Hayer, A.; De Halleux, V.; Koehler, A.; El-Garoughy, A.; Meijer, E. W.; Barbera, J.; Tant, J.; Levin, J.; Lehmann, M.; Gierschner, J.; Cornil, J.; Geerts, Y. H. *J. Phys. Chem. B* **2006**, *110*, 7653–7659.
(36) Chaudhuri, R.; Hsu, M.-Y.; Li, C.-W.; Wang, C.-I.; Chen, C.-J.; Lai, C. K.; Chen, L.-Y.; Liu, S.-H.; Wu, C.-C.; Liu, R.-S. *Org. Lett.* **2008**, *10*, 3053–3056.
(37) Kumar, S.; Varshney, S. K. *Mol. Cryst. Liq. Cryst.* **2002**, *378*, 59–64.
(38) Kumar, S.; Naidu, J. J.; Shankar Rao, D. S. *J. Mater. Chem.* **2002**, *12*, 1335–1341.
(39) Cristiano, R.; Gallardo, H.; Bortoluzzi, A. J.; Bechtold, I. H.; Campos, C. E. M.; Longo, R. L. *Chem. Commun.* **2008**, 5134–5136.
(40) Dhar, R.; Kumar, S.; Gupta, M.; Agrawal, V. K. *J. Mol. Liq.* **2008**, *141*, 19–24.
(41) Bisoyi, H. K.; Kumar, S. *New J. Chem.* **2008**, *32*, 1974–1980.
(42) Murschell, A. E.; Sutherland, T. C. *Langmuir* **2010**, *26*, 12859–12866.
(43) Negita, K.; Kawano, C.; Moriya, K. *Phys. Rev. E: Stat., Nonlinear, Soft Matter Phys.* **2004**, *70*, 021702/1–021702/5.
(44) Luo, J.; Zhao, B.; Shao, J.; Lim, K. A.; Chan, H. S. O.; Chi, C. *J. Mater. Chem.* **2009**, *19*, 8327–8334.
(45) Talarico, M.; Termine, R.; Garcia-Frutos, E. M.; Omenat, A.; Serrano, J. L.; Gomez-Lor, B.; Golemme, A. *Chem. Mater.* **2008**, *20*, 6589–6591.
(46) Kadam, J.; Faul, C. F. J.; Scherf, U. *Chem. Mater.* **2004**, *16*, 3867–3871.
(47) Boden, N.; Bushby, R. J.; Donovan, K.; Liu, Q.; Lu, Z.; Kreouzis, T.; Wood, A. *Liq. Cryst.* **2001**, *28*, 1739–1748.
(48) Ong, C. W.; Liao, S.-C.; Chang, T. H.; Hsu, H.-F. *Tetrahedron Lett.* **2003**, *44*, 1477–1480.
(49) Lehmann, M.; Kestemont, G.; Aspe, R. G.; Buess-Herman, C.; Koch, M. H. J.; Debije, M. G.; Piris, J.; de Haas, M. P.; Warman, J. M.; Watson, M. D.; Lemaur, V.; Cornil, J.; Geerts, Y. H.; Gearba, R.; Ivanov, D. A. *Chem.—Eur. J.* **2005**, *11*, 3349–3362.
(50) An, Z.; Yu, J.; Jones, S. C.; Barlow, S.; Yoo, S.; Domercq, B.; Prins, P.; Siebbeles, L. D. A.; Kippelen, B.; Marder, S. R. *Adv. Mater.* **2005**, *17*, 2580–2583.
(51) An, Z.; Yu, J.; Domercq, B.; Jones, S. C.; Barlow, S.; Kippelen, B.; Marder, S. R. *J. Mater. Chem.* **2009**, *19*, 6688–6698.
(52) Deibel, C.; Janssen, D.; Heremans, P.; De Cupere, V.; Geerts, Y.; Benkhedir, M. L.; Adriaenssens, G. J. *Org. Electron.* **2006**, *7*, 495–499.
(53) Sergeyev, S.; Debever, O.; Pouzet, E.; Geerts, Y. H. *J. Mater. Chem.* **2007**, *17*, 3002–3007.
(54) Kimura, M.; Narikawa, H.; Ohta, K.; Hanabusa, K.; Shirai, H.; Kobayashi, N. *Chem. Mater.* **2002**, *14*, 2711–2717.
(55) Donders, C. A.; Liu, S.-X.; Loosli, C.; Sanguinet, L.; Neels, A.; Decurtins, S. *Tetrahedron* **2006**, *62*, 3543–3549.
(56) Miao, J.; Zhu, L. *Soft Matter* **2010**, *6*, 2072–2079.
(57) Kroeze, J. E.; Koehorst, R. B. M.; Savenije, T. J. *Adv. Funct. Mater.* **2004**, *14*, 992–998.
(58) Qi, M.-H.; Liu, G.-F. *J. Mater. Chem.* **2003**, *13*, 2479–2484.
(59) Hu, J.; Zhang, D.; Jin, S.; Cheng, S. Z. D.; Harris, F. W. *Chem. Mater.* **2004**, *16*, 4912–4915.
(60) Leng, S.; Chan, L. H.; Jing, J.; Hu, J.; Moustafa, R. M.; Van Horn, R. M.; Graham, M. J.; Sun, B.; Zhu, M.; Jeong, K.-U.; Kaafarani, B. R.; Zhang, W.; Harris, F. W.; Cheng, S. Z. D. *Soft Matter* **2010**, *6*, 100–112.
(61) Wu, J.; Watson, M. D.; Zhang, L.; Wang, Z.; Müllen, K. *J. Am. Chem. Soc.* **2004**, *126*, 177–186.
(62) Feng, X.; Liu, M.; Pisula, W.; Takase, M.; Li, J.; Müllen, K. *Adv. Mater.* **2008**, *20*, 2684–2689.
(63) Wang, X.; Zhi, L.; Tsao, N.; Tomovic, Z.; Li, J.; Müllen, K. *Angew. Chem., Int. Ed.* **2008**, *47*, 2990–2992.
(64) Palma, M.; Levin, J.; Lemaur, V.; Liscio, A.; Palermo, V.; Cornil, J.; Geerts, Y.; Lehmann, M.; Samori, P. *Adv. Mater.* **2006**, *18*, 3313–3317.
(65) Kumaran, N.; Veneman, P. A.; Minch, B. A.; Mudalige, A.; Pemberton, J. E.; O'Brien, D. F.; Armstrong, N. R. *Chem. Mater.* **2010**, *22*, 2491–2501.
(66) Orlandi, S.; Muccioli, L.; Ricci, M.; Berardi, R.; Zannoni, C. *Chem. Cent. J.* **2007**, *1*.
(67) Dou, X.; Pisula, W.; Wu, J.; Bodwell, G. J.; Müllen, K. *Chem.—Eur. J.* **2008**, *14*, 240–249.
(68) Lavigueur, C.; Foster, E. J.; Williams, V. E. *J. Am. Chem. Soc.* **2008**, *130*, 11791–11800.
(69) Voisin, E.; Foster, E. J.; Rakotomalala, M.; Williams, V. E. *Chem. Mater.* **2009**, *21*, 3251–3261.
(70) Rego, J. A.; Kumar, S.; Ringsdorf, H. *Chem. Mater.* **1996**, *8*, 1402–1409.
(71) Warman, J. M.; de Haas, M. P.; Dicker, G.; Grozema, F. C.; Piris, J.; Debije, M. G. *Chem. Mater.* **2004**, *16*, 4600–4609.
(72) Dicker, G.; de Haas, M. P.; Siebbeles, L. D. A.; Warman, J. M. *Phys. Rev. B: Condens. Matter Mater. Phys.* **2004**, *70*, 045203/1–045203/8.
(73) Grozema, F. C.; Savenije, T. J.; Vermeulen, M. J. W.; Siebbeles, L. D. A.; Warman, J. M.; Meisel, A.; Neher, D.; Nothofer, H.-G.; Scherf, U. *Adv. Mater.* **2001**, *13*, 1627–1630.
(74) Warman, J. M.; van de Craats, A. M. *Mol. Cryst. Liq. Cryst.* **2003**, *396*, 41–72.
(75) van de Craats, A. M.; Warman, J. M. *Adv. Mater.* **2001**, *13*, 130–133.
(76) Ban, K.; Nishizawa, K.; Ohta, K.; van de Craats, A. M.; Warman, J. M.; Yamamoto, I.; Shirai, H. *J. Mater. Chem.* **2001**, *11*, 321–331.
(77) Debije, M. G.; Piris, J.; De Haas, M. P.; Warman, J. M.; Tomovic, Z.; Simpson, C. D.; Watson, M. D.; Müllen, K. *J. Am. Chem. Soc.* **2004**, *126*, 4641–4645.
(78) Warman, J. M.; Piris, J.; Pisula, W.; Kastler, M.; Wasserfallen, D.; Müllen, K. *J. Am. Chem. Soc.* **2005**, *127*, 14257–14262.
(79) Adam, D.; Schuhmacher, P.; Simmerer, J.; Haeussling, L.; Siemensmeyer, K.; Etzbach, K. H.; Ringsdorf, H.; Haarer, D. *Nature* **1994**, *371*, 141–143.
(80) Borsenberger, P. M.; Magin, E. H.; van der Auweraer, M.; de Schryver, F. C. *Phys. Status Solidi A* **1993**, *140*, 9–47.
(81) Poplavskyy, D.; Nelson, J. *J. Appl. Phys.* **2003**, *93*, 341–346.
(82) Rybak, A.; Pfleger, J.; Jung, J.; Pavlik, M.; Glowacki, I.; Ulanski, J.; Tomovic, Z.; Müllen, K.; Geerts, Y. *Synth. Met.* **2006**, *156*, 302–309.
(83) Blom, P. W. M.; de Jong, M. J. M.; van Munster, M. G. *Phys. Rev. B: Condens. Matter* **1997**, *55*, R656–R659.
(84) Bozano, L.; Carter, S. A.; Scott, J. C.; Malliaras, G. G.; Brock, P. J. *Appl. Phys. Lett.* **1999**, *74*, 1132–1134.
(85) Shen, Y.; Klein, M. W.; Jacobs, D. B.; Campbell Scott, J.; Malliaras, G. G. *Phys. Rev. Lett.* **2001**, *86*, 3867–3870.
(86) Mihailetchi, V. D.; van Duren, J. K. J.; Blom, P. W. M.; Hummelen, J. C.; Janssen, R. A. J.; Kroon, J. M.; Rispens, M. T.; Verhees, W. J. H.; Wienk, M. M. *Adv. Funct. Mater.* **2003**, *13*, 43–46.
(87) Babel, A.; Jenekhe, S. A. *J. Am. Chem. Soc.* **2003**, *125*, 13656–13657.
(88) Podzorov, V.; Sysoev, S. E.; Loginova, E.; Pudalov, V. M.; Gershenson, M. E. *Appl. Phys. Lett.* **2003**, *83*, 3504–3506.
(89) Kaafarani, B. R.; Lucas, L. A.; Wex, B.; Jabbour, G. E. *Tetrahedron Lett.* **2007**, *48*, 5995–5998.
(90) Domercq, B.; Yu, J.; Kaafarani, B. R.; Kondo, T.; Yoo, S.; Haddock, J. N.; Barlow, S.; Marder, S. R.; Kippelen, B. *Mol. Cryst. Liq. Cryst.* **2008**, *481*, 80–93.
(91) Pisula, W.; Tomovic, Z.; Simpson, C.; Kastler, M.; Pakula, T.; Müllen, K. *Chem. Mater.* **2005**, *17*, 4296–4303.
(92) Pisula, W.; Kastler, M.; Wasserfallen, D.; Mondeshki, M.; Piris, J.; Schnell, I.; Müllen, K. *Chem. Mater.* **2006**, *18*, 3634–3640.
(93) Holt, L. A.; Bushby, R. J.; Evans, S. D.; Burgess, A.; Seeley, G. *J. Appl. Phys.* **2008**, *103*, 063712/1–063712/7.

(94) Leng, S.; Wex, B.; Chan, L. H.; Graham, M. J.; Jin, S.; Jing, A. J.; Jeong, K.-U.; Van Horn, R. M.; Sun, B.; Zhu, M.; Kaafarani, B. R.; Cheng, S. Z. D. *J. Phys. Chem. B* **2009**, *113*, 5403–5411.
(95) Duzhko, V.; Semyonov, A.; Twieg, R. J.; Singer, K. D. *Phys. Rev. B: Condens. Matter Mater. Phys.* **2006**, *73*, 064201/1–064201/5.
(96) Iino, H.; Takayashiki, Y.; Hanna, J.-i.; Bushby, R. J.; Haarer, D. *Appl. Phys. Lett.* **2005**, *87*, 192105/1–192105/3.
(97) Sienkowska, M. J.; Monobe, H.; Kaszynski, P.; Shimizu, Y. *J. Mater. Chem.* **2007**, *17*, 1392–1398.
(98) Fujikake, H.; Murashige, T.; Sugibayashi, M.; Ohta, K. *Appl. Phys. Lett.* **2004**, *85*, 3474–3476.
(99) Mizoshita, N.; Monobe, H.; Inoue, M.; Ukon, M.; Watanabe, T.; Shimizu, Y.; Hanabusa, K.; Kato, T. *Chem. Commun.* **2002**, 428–429.
(100) Gearba, R. I.; Lehmann, M.; Levin, J.; Ivanov, D. A.; Koch, M. H. J.; Barbera, J.; Debije, M. G.; Piris, J.; Geerts, Y. H. *Adv. Mater.* **2003**, *15*, 1614–1618.
(101) Rohr, U.; Kohl, C.; Müllen, K.; van de Craats, A.; Warman, J. *J. Mater. Chem.* **2001**, *11*, 1789–1799.
(102) Feng, X.; Marcon, V.; Pisula, W.; Hansen, M. R.; Kirkpatrick, J.; Grozema, F.; Andrienko, D.; Kremer, K.; Müllen, K. *Nat. Mater.* **2009**, *8*, 421–426.
(103) Kaefer, D.; Bashir, A.; Dou, X.; Witte, G.; Müllen, K.; Woell, C. *Adv. Mater.* **2010**, *22*, 384–388.
(104) Yamamoto, Y.; Fukushima, T.; Suna, Y.; Ishii, N.; Saeki, A.; Seki, S.; Tagawa, S.; Taniguchi, M.; Kawai, T.; Aida, T. *Science* **2006**, *314*, 1761–1764.
(105) Zhang, G.; Jin, W.; Fukushima, T.; Kosaka, A.; Ishii, N.; Aida, T. *J. Am. Chem. Soc.* **2007**, *129*, 719–722.
(106) Mynar, J. L.; Yamamoto, T.; Kosaka, A.; Fukushima, T.; Ishii, N.; Aida, T. *J. Am. Chem. Soc.* **2008**, *130*, 1530–1531.
(107) Zhang, W.; Jin, W.; Fukushima, T.; Ishii, N.; Aida, T. *Angew. Chem., Int. Ed.* **2009**, *48*, 4747–4750.
(108) Kouwer, P. H. J.; van den Berg, O.; Jager, W. F.; Mijs, W. J.; Picken, S. J. *Macromolecules* **2002**, *35*, 2576–2582.
(109) Kouwer, P. H. J.; Jager, W. F.; Mijs, W. J.; Picken, S. J. *Macromolecules* **2002**, *35*, 4322–4329.
(110) Hughes, J. R.; Luckhurst, G. R.; Praefcke, K.; Singer, D.; Tearle, W. M. *Mol. Cryst. Liq. Cryst.* **2003**, *396*, 187–225.
(111) Bushby, R. J.; Donovan, K. J.; Kreouzis, T.; Lozman, O. R. *Opto-Electron. Rev.* **2005**, *13*, 269–279.
(112) Percec, V.; Glodde, M.; Bera, T. K.; Miura, Y.; Shiyanovskaya, I.; Singer, K. D.; Balagurusamy, V. S. K.; Heiney, P. A.; Schnell, I.; Rapp, A.; Spiess, H. W.; Hudson, S. D.; Duan, H. *Nature* **2002**, *419*, 384–387.
(113) Weck, M.; Dunn, A. R.; Matsumoto, K.; Coates, G. W.; Lobkovsky, E. B.; Grubbs, R. H. *Angew. Chem., Int. Ed.* **1999**, *38*, 2741–2745.
(114) Kumar, P. S.; Kumar, S.; Lakshminarayanan, V. *J. Phys. Chem. B* **2008**, *112*, 4865–4869.
(115) Pisula, W.; Kastler, M.; Wasserfallen, D.; Robertson, J. W. F.; Nolde, F.; Kohl, C.; Müllen, K. *Angew. Chem., Int. Ed.* **2006**, *45*, 819–823.
(116) Pisula, W.; Tomovic, Z.; El Hamaoui, B.; Watson, M. D.; Pakula, T.; Müllen, K. *Adv. Funct. Mater.* **2005**, *15*, 893–904.
(117) Gearba, R. I.; Anokhin, D. V.; Bondar, A. I.; Bras, W.; Jahr, M.; Lehmann, M.; Ivanov, D. A. *Adv. Mater.* **2007**, *19*, 815–820.
(118) Grelet, E.; Dardel, S.; Bock, H.; Goldmann, M.; Lacaze, E.; Nallet, F. *Eur. Phys. J. E.: Soft Matter Biol. Phys.* **2010**, *31*, 343−349.
(119) Liu, C.-y.; Fechtenkötter, A.; Watson, M. D.; Müllen, K.; Bard, A. J. *Chem. Mater.* **2003**, *15*, 124–130.
(120) Sergeyev, S.; Levin, J.; Balandier, J.-Y.; Pouzet, E.; Geerts, Y. H. *Mendeleev Commun.* **2009**, *19*, 185–186.
(121) Sirringhaus, H.; Brown, P. J.; Friend, R. H.; Nielsen, M. M.; Bechgaard, K.; Langeveld-Voss, B. M. W.; Spiering, A. J. H.; Janssen, R. A. J.; Meijer, E. W.; Herwig, P.; De Leeuw, D. M. *Nature* **1999**, *401*, 685–688.
(122) Sirringhaus, H.; Wilson, R. J.; Friend, R. H.; Inbasekaran, M.; Wu, W.; Woo, E. P.; Grell, M.; Bradley, D. D. C. *Appl. Phys. Lett.* **2000**, *77*, 406–408.
(123) Eichhorn, S. H.; Adavelli, A.; Li, H. S.; Fox, N. *Mol. Cryst. Liq. Cryst.* **2003**, *397*, 347–358.
(124) Tracz, A.; Jeszka, J. K.; Watson, M. D.; Pisula, W.; Müllen, K.; Pakula, T. *J. Am. Chem. Soc.* **2003**, *125*, 1682–1683.
(125) Pisula, W.; Menon, A.; Stepputat, M.; Lieberwirth, I.; Kolb, U.; Tracz, A.; Sirringhaus, H.; Pakula, T.; Müllen, K. *Adv. Mater.* **2005**, *17*, 684–689.
(126) Piris, J.; Pisula, W.; Warman, J. M. *Synth. Met.* **2004**, *147*, 85–89.
(127) Piris, J.; Pisula, W.; Tracz, A.; Pakula, T.; Müllen, K.; Warman, J. *Liq. Cryst.* **2004**, *31*, 993–996.
(128) Liu, C.-Y.; Bard, A. J. *Chem. Mater.* **2000**, *12*, 2353–2362.
(129) Laursen, B. W.; Norgaard, K.; Reitzel, N.; Simonsen, J. B.; Nielsen, C. B.; Als-Nielsen, J.; Bjornholm, T.; Solling, T. I.; Nielsen, M. M.; Bunk, O.; Kjaer, K.; Tchebotareva, N.; Watson, M. D.; Müllen, K.; Piris, J. *Langmuir* **2004**, *20*, 4139–4146.
(130) Reitzel, N.; Hassenkam, T.; Balashev, K.; Jensen, T. R.; Howes, P. B.; Kjaer, K.; Fechtenkotter, A.; Tchebotareva, N.; Ito, S.; Müllen, K.; Bjornholm, T. *Chem.—Eur. J.* **2001**, *7*, 4894–4901.
(131) Smolenyak, P. E.; Osburn, E. J.; Chen, S. Y.; Chau, L. K.; O'Brien, D. F.; Armstrong, N. R. *Langmuir* **1997**, *13*, 6568–6576.
(132) Tsukruk, V. V.; Bengs, H.; Ringsdorf, H. *Langmuir* **1996**, *12*, 754–757.
(133) Bunk, O.; Nielsen, M. M.; Solling, T. I.; van de Craats, A. M.; Stutzmann, N. *J. Am. Chem. Soc.* **2003**, *125*, 2252–2258.
(134) Zimmermann, S.; Wendorff, J. H.; Weder, C. *Chem. Mater.* **2002**, *14*, 2218–2223.
(135) Charlet, E.; Grelet, E. *Phys. Rev. E: Stat., Nonlinear, Soft Matter Phys.* **2008**, *78*, 041707/1–041707/8.
(136) Mouthuy, P.-O.; Melinte, S.; Geerts, Y. H.; Jonas, A. M. *Nano Lett.* **2007**, *7*, 2627–2632.
(137) Ge, J. J.; Hong, S.-C.; Tang, B. Y.; Li, C. Y.; Zhang, D.; Bai, F.; Mansdorf, B.; Harris, F. W.; Yang, D.; Shen, Y.-R.; Cheng, S. Z. D. *Adv. Funct. Mater.* **2003**, *13*, 718–725.
(138) Archambeau, S.; Seguy, I.; Jolinat, P.; Farenc, J.; Destruel, P.; Nguyen, T. P.; Bock, H.; Grelet, E. *Appl. Surf. Sci.* **2006**, *253*, 2078–2086.
(139) Yoshio, M.; Kagata, T.; Hoshino, K.; Mukai, T.; Ohno, H.; Kato, T. *J. Am. Chem. Soc.* **2006**, *128*, 5570–5577.
(140) Hoogboom, J.; Garcia, P. M. L.; Otten, M. B. J.; Elemans, J. A. A. W.; Sly, J.; Lazarenko, S. V.; Rasing, T.; Rowan, A. E.; Nolte, R. J. M. *J. Am. Chem. Soc.* **2005**, *127*, 11047–11052.
(141) Monobe, H.; Kiyohara, K.; Heya, M.; Awazu, K.; Shimizu, Y. *Mol. Cryst. Liq. Cryst.* **2003**, *397*, 359–365.
(142) Monobe, H.; Kiyohara, K.; Terasawa, N.; Heya, M.; Awazu, K.; Shimizu, Y. *Adv. Funct. Mater.* **2003**, *13*, 919–924.
(143) Monobe, H.; Kiyohara, K.; Shimizu, Y.; Heya, M.; Awazu, K. *Mol. Cryst. Liq. Cryst.* **2004**, *410*, 557–566.
(144) Monobe, H.; Shimizu, Y. *Kino Zairyo* **2005**, *25*, 23–30.
(145) Monobe, H.; Shimizu, Y.; Heya, M.; Awazu, K. *Mol. Cryst. Liq. Cryst.* **2005**, *443*, 211–217.
(146) Shimizu, Y.; Monobe, H.; Heya, M.; Awazu, K. *Mol. Cryst. Liq. Cryst.* **2005**, *441*, 287–295.
(147) Shimizu, Y.; Monobe, H.; Heya, M.; Awazu, K. *Mol. Cryst. Liq. Cryst.* **2005**, *443*, 49–58.
(148) Monobe, H.; Terasawa, N.; Shimizu, Y.; Kiyohara, K.; Heya, M.; Awazu, K. *Mol. Cryst. Liq. Cryst.* **2005**, *437*, 1325–1332.
(149) Monobe, H.; Hori, H.; Heya, M.; Awazu, K.; Shimizu, Y. *Thin Solid Films* **2006**, *499*, 259–262.
(150) Monobe, H.; Awazu, K.; Shimizu, Y. *Adv. Mater.* **2006**, *18*, 607–610.
(151) Monobe, H.; Awazu, K.; Shimizu, Y. *Thin Solid Films* **2009**, *518*, 762–766.
(152) Lee, J.-H.; Choi, S.-M.; Pate, B. D.; Chisholm, M. H.; Han, Y.-S. *J. Mater. Chem.* **2006**, *16*, 2785–2791.
(153) Lee, J.-H.; Kim, H.-S.; Pate, B. D.; Choi, S.-M. *Phys. B* **2006**, *385−386*, 798–800.
(154) Kim, H.-S.; Choi, S.-M.; Lee, J.-H.; Busch, P.; Koza, S. J.; Verploegen, E. A.; Pate, B. D. *Adv. Mater.* **2008**, *20*, 1105–1109.
(155) Shklyarevskiy, I. O.; Jonkheijm, P.; Stutzmann, N.; Wasserberg, D.; Wondergem, H. J.; Christianen, P. C. M.; Schenning, A. P. H. J.; De Leeuw, D. M.; Tomovic, Z.; Wu, J.; Müllen, K.; Maan, J. C. *J. Am. Chem. Soc.* **2005**, *127*, 16233–16237.
(156) Pouzet, E.; De Cupere, V.; Heintz, C.; Andreasen, J. W.; Breiby, D. W.; Nielsen, M. M.; Viville, P.; Lazzaroni, R.; Gbabode, G.; Geerts, Y. H. *J. Phys. Chem. C* **2009**, *113*, 14398–14406.
(157) Zucchi, G.; Donnio, B.; Geerts, Y. H. *Chem. Mater.* **2005**, *17*, 4273–4277.
(158) Schweicher, G.; Gbabode, G.; Quist, F.; Debever, O.; Dumont, N.; Sergeyev, S.; Geerts, Y. H. *Chem. Mater.* **2009**, *21*, 5867–5874.
(159) Zucchi, G.; Viville, P.; Donnio, B.; Vlad, A.; Melinte, S.; Mondeshki, M.; Graf, R.; Spiess, H. W.; Geerts, Y. H.; Lazzaroni, R. *J. Phys. Chem. B* **2009**, *113*, 5448–5457.
(160) Thiebaut, O.; Bock, H.; Grelet, E. *J. Am. Chem. Soc.* **2010**, *132*, 6886–6887.
(161) De Luca, G.; Liscio, A.; Melucci, M.; Schnitzler, T.; Pisula, W.; Clark, C. G.; Scolaro, L. M.; Palermo, V.; Müllen, K.; Samori, P. *J. Mater. Chem.* **2010**, *20*, 71–82.
(162) Arikainen, E. O.; Boden, N.; Bushby, R. J.; Lozman, O. R.; Vinter, J. G.; Wood, A. *Angew. Chem., Int. Ed.* **2000**, *39*, 2333–2336.
(163) Lydon, J. *Curr. Opin. Colloid Interface Sci.* **2004**, *8*, 480–490.
(164) Bushby, R. J.; Hamley, I. W.; Liu, Q.; Lozman, O. R.; Lydon, J. E. *J. Mater. Chem.* **2005**, *15*, 4429–4434.
(165) Geerts, Y. H.; Debever, O.; Amato, C.; Sergeyev, S. Beilstein J. Org. Chem. **2009**, *5*.
(166) Orlandi, S.; Muccioli, L.; Ricci, M.; Zannoni, C. *Soft Matter* **2009**, *5*, 4484–4491.
(167) Nuckolls, C.; Shao, R.; Jang, W.-G.; Clark, N. A.; Walba, D. M.; Katz, T. J. *Chem. Mater.* **2002**, *14*, 773–776.
(168) Bushey, M. L.; Nguyen, T.-Q.; Nuckolls, C. *J. Am. Chem. Soc.* **2003**, *125*, 8264–8269.
(169) Gorecka, E.; Pociecha, D.; Mieczkowski, J.; Matraszek, J.; Guillon, D.; Donnio, B. *J. Am. Chem. Soc.* **2004**, *126*, 15946–15947.
(170) Kishikawa, K.; Nakahara, S.; Nishikawa, Y.; Kohmoto, S.; Yamamoto, M. *J. Am. Chem. Soc.* **2005**, *127*, 2565–2571.
(171) Takezoe, H.; Kishikawa, K.; Gorecka, E. *J. Mater. Chem.* **2006**, *16*, 2412–2416.
(172) Calo, A.; Stoliar, P.; Cavallini, M.; Sergeyev, S.; Geerts, Y. H.; Biscarini, F. *J. Am. Chem. Soc.* **2008**, *130*, 11953–11958.
(173) Shimura, H.; Yoshio, M.; Hamasaki, A.; Mukai, T.; Ohno, H.; Kato, T. *Adv. Mater.* **2009**, *21*, 1591–1594.

(174) Miyajima, D.; Tashiro, K.; Araoka, F.; Takezoe, H.; Kim, J.; Kato, K.; Takata, M.; Aida, T. *J. Am. Chem. Soc.* **2009**, *131*, 44–45.
(175) Bramble, J. P.; Tate, D. J.; Revill, D. J.; Sheikh, K. H.; Henderson, J. R.; Liu, F.; Zeng, X.; Ungar, G.; Bushby, R. J.; Evans, S. D. *Adv. Funct. Mater.* **2010**, *20*, 914–920.
(176) Grelet, E.; Bock, H. *Europhys. Lett.* **2006**, *73*, 712–718.
(177) Charlet, E.; Grelet, E.; Brettes, P.; Bock, H.; Saadaoui, H.; Cisse, L.; Destruel, P.; Gherardi, N.; Seguy, I. *Appl. Phys. Lett.* **2008**, *92*, 024107/1–024107/3.
(178) Terasawa, N.; Monobe, H.; Kiyohara, K.; Shimizu, Y. *Chem. Commun.* **2003**, 1678–1679.
(179) Kouwer, P. H. J.; Picken, S. J.; Mehl, G. H. *J. Mater. Chem.* **2007**, *17*, 4196–4203.
(180) Kato, T.; Mizoshita, N.; Moriyama, M.; Kitamura, T. *Top. Curr. Chem.* **2005**, *256*, 219–236.
(181) Hirai, Y.; Monobe, H.; Mizoshita, N.; Moriyama, M.; Hanabusa, K.; Shimizu, Y.; Kato, T. *Adv. Funct. Mater.* **2008**, *18*, 1668–1675.
(182) Furumi, S.; Ichimura, K. *Kino Zairyo* **2005**, *25*, 15–22.
(183) Furumi, S.; Ichimura, K. *J. Phys. Chem. B* **2007**, *111*, 1277–1287.
(184) Furumi, S.; Kidowaki, M.; Ogawa, M.; Nishiura, Y.; Ichimura, K. *J. Phys. Chem. B* **2005**, *109*, 9245–9254.
(185) Cavallini, M.; Calo, A.; Stoliar, P.; Kengne, J. C.; Martins, S.; Matacotta, F. C.; Quist, F.; Gbabode, G.; Dumont, N.; Geerts, Y. H.; Biscarini, F. *Adv. Mater.* **2009**, *21*, 4688–4691.
(186) Cavallini, M.; Bergenti, I.; Milita, S.; Ruani, G.; Salitros, I.; Qu, Z.-R.; Chandrasekar, R.; Ruben, M. *Angew. Chem., Int. Ed.* **2008**, *47*, 8596–8600.
(187) Serban, D. A.; Greco, P.; Melinte, S.; Vlad, A.; Dutu, C. A.; Zacchini, S.; Iapalucci, M. C.; Biscarini, F.; Cavallini, M. *Small* **2009**, *5*, 1117–1122.
(188) De Cupere, V.; Tant, J.; Viville, P.; Lazzaroni, R.; Osikowicz, W.; Salaneck, W. R.; Geerts, Y. H. *Langmuir* **2006**, *22*, 7798–7806.
(189) Ishi-i, T.; Kuwahara, R.; Takata, A.; Jeong, Y.; Sakurai, K.; Mataka, S. *Chem.—Eur. J.* **2006**, *12*, 763–776.
(190) Minch, B. A.; Xia, W.; Donley, C. L.; Hernandez, R. M.; Carter, C.; Carducci, M. D.; Dawson, A.; O'Brien, D. F.; Armstrong, N. R. *Chem. Mater.* **2005**, *17*, 1618–1627.
(191) Wu, J.; Watson, M. D.; Zhang, L.; Wang, Z.; Müllen, K. *J. Am. Chem. Soc.* **2004**, *126*, 177–186.
(192) Schmidt-Mende, L.; Watson, M.; Müllen, K.; Friend, R. H. *Mol. Cryst. Liq. Cryst.* **2003**, *396*, 73–90.
(193) Ba, C.-Y.; Shen, Z.-R.; Gu, H.-W.; Guo, G.-Q.; Xie, P.; Zhang, R.-B.; Zhu, C.-F.; Wan, L.-J.; Li, F.-Y.; Huang, C.-H. *Liq. Cryst.* **2003**, *30*, 391–397.
(194) van Gorp, J. J.; Vekemans, J. A. J. M.; Meijer, E. W. *J. Am. Chem. Soc.* **2002**, *124*, 14759–14769.
(195) Schoenherr, H.; Manickam, M.; Kumar, S. *Langmuir* **2002**, *18*, 7082–7085.
(196) Kevenhoerster, B.; Kopitzke, J.; Seifert, A. M.; Tsukruk, V.; Wendorff, J. H. *Adv. Mater.* **1999**, *11*, 246–250.
(197) Schoenherr, H.; Kremer, F. J. B.; Kumar, S.; Rego, J. A.; Wolf, H.; Ringsdorf, H.; Jaschke, M.; Butt, H. J.; Bamberg, E. *J. Am. Chem. Soc.* **1996**, *118*, 13051–13057.
(198) Piot, L.; Marie, C.; Feng, X.; Müllen, K.; Fichou, D. *Adv. Mater.* **2008**, *20*, 3854–3858.
(199) Treier, M.; Ruffieux, P.; Groening, P.; Xiao, S.; Nuckolls, C.; Fasel, R. *Chem. Commun.* **2008**, 4555–4557.
(200) Palma, M.; Pace, G.; Roussel, O.; Geerts, Y.; Samori, P. *Aust. J. Chem.* **2006**, *59*, 376–380.
(201) De Feyter, S.; De Schryver, F. C. *J. Phys. Chem. B* **2005**, *109*, 4290–4302.
(202) Jaeckel, F.; Watson, M. D.; Müllen, K.; Rabe, J. P. *Phys. Rev. Lett.* **2004**, *92*, 188303/1–188303/4.
(203) Tchebotareva, N.; Yin, X.; Watson, M. D.; Samori, P.; Rabe, J. P.; Müllen, K. *J. Am. Chem. Soc.* **2003**, *125*, 9734–9739.
(204) Cornil, J.; Lemaur, V.; Calbert, J.-P.; Brédas, J.-L. *Adv. Mater.* **2002**, *14*, 726–729.
(205) Lemaur, V.; da Silva Filho, D. A.; Coropceanu, V.; Lehmann, M.; Geerts, Y.; Piris, J.; Debije, M. G.; van de Craats, A. M.; Senthilkumar, K.; Siebbeles, L. D. A.; Warman, J. M.; Brédas, J.-L.; Cornil, J. *J. Am. Chem. Soc.* **2004**, *126*, 3271–3279.
(206) Kirkpatrick, J.; Marcon, V.; Kremer, K.; Nelson, J.; Andrienko, D. *Phys. Status Solidi B* **2008**, *245*, 835–838.
(207) Andrienko, D.; Kirkpatrick, J.; Marcon, V.; Nelson, J.; Kremer, K. *Phys. Status Solidi B* **2008**, *245*, 830–834.
(208) Olivier, Y.; Muccioli, L.; Lemaur, V.; Geerts, Y. H.; Zannoni, C.; Cornil, J. *J. Phys. Chem. B* **2009**, *113*, 14102–14111.
(209) Seguy, I.; Jolinat, P.; Destruel, P.; Farenc, J.; Mamy, R.; Bock, H.; Ip, J.; Nguyen, T. P. *J. Appl. Phys.* **2001**, *89*, 5442–5448.
(210) Schmidt-Mende, L.; Fechtenkötter, A.; Müllen, K.; Moons, E.; Friend, R. H.; MacKenzie, J. D. *Science* **2001**, *293*, 1119–1122.
(211) Li, L.; Kang, S.-W.; Harden, J.; Sun, Q.; Zhou, X.; Dai, L.; Jakli, A.; Kumar, S.; Li, Q. *Liq. Cryst.* **2008**, *35*, 233–239.
(212) Jung, J.; Rybak, A.; Slazak, A.; Bialecki, S.; Miskiewicz, P.; Glowacki, I.; Ulanski, J.; Rosselli, S.; Yasuda, A.; Nelles, G.; Tomovic, Z.; Watson, M. D.; Müllen, K. *Synth. Met.* **2005**, *155*, 150–156.
(213) Schmidtke, J. P.; Friend, R. H.; Kastler, M.; Müllen, K. *J. Chem. Phys.* **2006**, *124*, 174704/1–174704/6.
(214) Schmidt-Mende, L.; Fechtenkötter, A.; Müllen, K.; Friend, R. H.; MacKenzie, J. D. *Phys. E* **2002**, *14*, 263–267.
(215) Oukachmih, M.; Destruel, P.; Seguy, I.; Ablart, G.; Jolinat, P.; Archambeau, S.; Mabiala, M.; Fouet, S.; Bock, H. *Sol. Energy Mater. Sol. Cells* **2005**, *85*, 535–543.
(216) Tsao, H. N.; Pisula, W.; Liu, Z.; Osikowicz, W.; Salaneck, W. R.; Müllen, K. *Adv. Mater.* **2008**, *20*, 2715–2719.
(217) Chesterfield, R. J.; McKeen, J. C.; Newman, C. R.; Ewbank, P. C.; Da Silva Filho, D. A.; Brédas, J.-L.; Miller, L. L.; Mann, K. R.; Frisbie, C. D. *J. Phys. Chem. B* **2004**, *108*, 19281–19292.
(218) Dong, S.; Tian, H.; Song, D.; Yang, Z.; Yan, D.; Geng, Y.; Wang, F. *Chem. Commun.* **2009**, 3086–3088.
(219) Hoang, M. H.; Cho, M. J.; Kim, K. H.; Cho, M. Y.; Joo, J.-s.; Choi, D. H. *Thin Solid Films* **2009**, *518*, 501–506.
(220) Guo, X.; Xiao, S.; Myers, M.; Miao, Q.; Steigerwald, M. L.; Nuckolls, C. *Proc. Natl. Acad. Sci. U.S.A.* **2009**, *106*, 691–696.
(221) Mori, H. *Jpn. J. Appl. Phys., Part 1* **1997**, *36*, 1068–1072.
(222) Leenhouts, F. *Jpn. J. Appl. Phys., Part 2* **2000**, *39*, L741–L743.
(223) Kawata, K. *Chem. Rec.* **2002**, *2*, 59–80.